CHALMERS

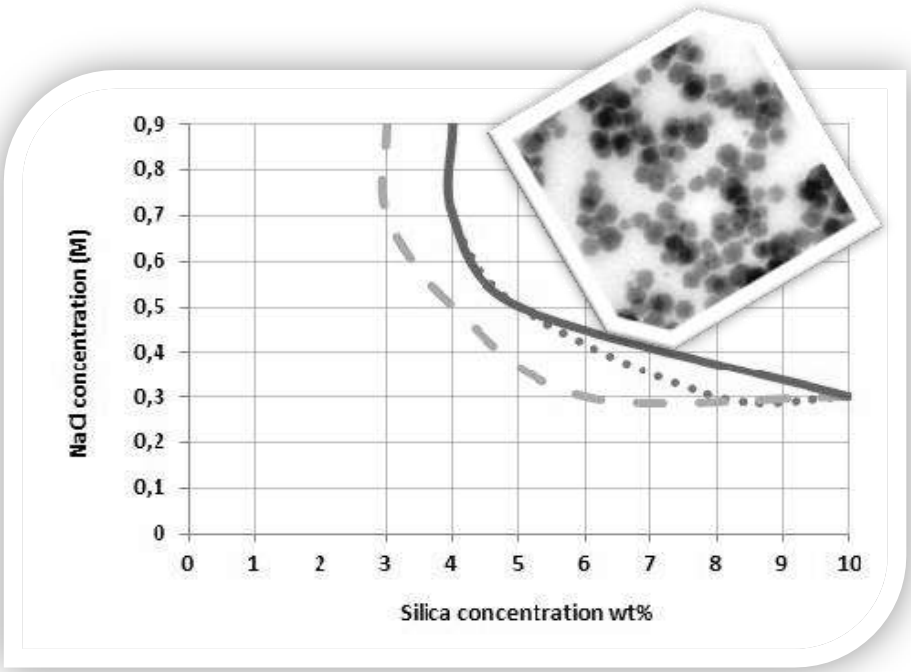

Microstructure and Gel Kinetics in Silica Composite Gels

for Application in Mass Transport Research

Master of Science Thesis of Material and Nanotechnology Program

SEYED MOJTABA SIAHPOOSH

Department of Chemical and biological Engineering
Division of Applied Surface Chemistry
CHALMERS UNIVERSITY OF TECHNOLOGY
Göteborg, Sweden, December 2011

Contents

Abstract

Mass transport phenomenon is of importance in numerous processes in our everyday life and is a crucial factor in the design of many materials. This work focuses on design, synthesis and characterization of a gel model material composed of colloid silica by itself or in combination with nano cellulose. These materials will later be used to study how material nano and micro structure control diffusion and flow within materials. The pseudo-phase behavior and kinetics of gelation in unstable colloidal silica/nano cellulose (NCC) sols has been studied in different pHs and salt concentrations to generate a library of structures for characterization. Generally, the minimum silica concentration for gel formation for the studied colloidal silica system was 3 wt% and minimum NaCl concentration was 0.2-0.3 M. When varying pH, NaCl or NCC concentration the silica system showed no significant changes in silica structure as found by TEM, indicating a robust structure formation by the colloidal silica. The interaction between silica and NCC was investigated by adsorption studies by the QCM-D method. As expected, it was found that silica only adsorb onto NCC covered surfaces at around pH 2, when silica has reached its isoelectric point. Some initial studies with 1H-NMR diffusometry was done and as expected it was found that an increasing volume fraction gives a linear reduction in the diffusion. However the decrease was larger than expected theoretically from pure obstruction, probably as results of some water binding to the silica surface. There was also an indication that a decrease in pH increased the diffusion slightly. The changes in diffusion constants were overall small.

Chapter 1 Background

1.1. Mass transport in soft biomaterials, what is it and why is it important?

Transport phenomenon in soft materials is one of the essential topics for material scientists and material designers. As an example mass transport is of crucial importance in biomaterial science when a drug is to have a customized release profile from a biomaterial. In addition, mass transport properties are very important in wound healing. For instance, production of a foam dressing with effective absorbing qualities is important in wound healing. This dressing should uptake wound liquids efficiently. Mass transport is of crucial importance also in other industries for processes such as film formation, ceramics processing, as well as production of food stuffs [1]. Controlling transport of oxygen and humidity through the barrier films and through the different food materials is another challenging subject for the food industry. Thus, research is this area offers many challenges and possibilities for improvement of materials, providing new opportunities for increase industrial profitability [2].

1.2. The SuMo Biomaterial Organization

This project was conducted within *SuMo Biomaterials*, a VINN EXCELLENCE centre financed by VINNOVA. *SuMo* is an academic and industrial joint effort with a focus on understanding and developing properties of soft biomaterials. *SuMo* tries to achieve predictability with respect to designing materials with specific mass transport profiles. To achieve this, collaboration between different scientific disciplines is necessary; therefore, *SuMo* is divided to four research modules that work in concert with each other. In short the *diffusion & flow module* focuses on experimental characterization of mass transport on various length and time-scales. The *material structure module* focuses on static and dynamic microstructure characterization at several length scales. In the *mathematical & computer modeling module*, modeling of both microstructure and mass transport is the main goal. Finally, *the material design module* constructs material with structures varying from millimeters to nanometers with the purpose of achieving understanding and predictive design in mass transport properties in different soft matter systems [1].The project described in this thesis is part of the *material structure module* in *SuMo.*

Chapter 2 Introduction

2.1. Mass Transport

When a cube of sugar is added to a cup of still coffee, it will start to dissolve into its individual sugar molecules (carbohydrates). Then, carbohydrate molecules will spread throughout the coffee until the concentration of sugar will be completely uniform. In this simple everyday example, two mechanisms have contribution in sweetening of the coffee and dispersion of sugar molecules in the liquid. The first mechanism of mass transport is *diffusion.* In this case is driven by the differences in concentration of sugar in different regions of the cup. Diffusion continues until the concentration gradient becomes zero everywhere. Diffusion is slow and in some system it could take several years or more until the concentration would be uniform everywhere. Diffusion of material is often slow in solids and equilibrium conditions are not often reachable and sensible. In the previous example diffusion rate of sugar molecules into the glass/ceramic cup material is most likely very slow and it may takes many years for penetration of a sugar molecule into the cup wall [2].

The second mechanism in mass transfer is *flow* which involves the bulk motion of molecules and contains larger scales of mass transferring. If the coffee cup is mixed with the spoon in the example above, huge numbers of carbohydrate molecules will be carried from the bottom region to the other regions of the cup where the cube of sugar has melted, to other regions of the cup. There are two types of flow for a fluid (liquid or gas). It can be laminar flow or turbulent flow. In laminar flow each particle in the fluid follows a streamline and transportation of particles in the laminar flow is predictable but in the turbulent flow it is more chaotic in nature with eddies and other types of complex flow behavior. Flow measurement was not within the scope of the current study but will most likely be studied in the future work.

2.1.1. Diffusion

There are at least two approaches in studying and understanding diffusion in literature: One is phenomenological approach which was explained previously by a simple every day example but there is also a second approach done with mathematics. This approach is based on “random walk” of diffusive particles in a continuous phase [3]. Thomas Graham did the first systematic study about diffusion phenomenon but the first quantitative experiment was done by Adolf Fick. He proposed his quantitative law on 1855 in Zurich when he was only 26 years old. Fick found similarity between diffusion of matter, conduction of heat and conduction of electricity. Therefore, his mathematical formula was similar to Fourier’s law for heat conduction and Ohm’s law for electricity. It is a partial derivative equation of the second degree [3]:

Flux of mass is proportional to gradient of its concentration (y in formula) with the proportionality factor k, which is a constant dependent upon the nature of the material. The rate of diffusion is directly proportional to the membrane surface area and the concentration gradient and is inversely proportional to the membrane thickness:

This equation (equation 2) is *Fick's law* which refers to one-directional diffusion, in the z-direction where:

J_A = molecular diffusion flux (dimension: kg-mole/m^2.s)

D_{AB}= diffusion coefficient of A in a mixture of A and B (dimension: m^2/s)

dC_A/dz = concentration gradient (dimension: kg-mole.m^{-3}/m)

Self-diffusion and restricted diffusion

Self-diffusion is the translational motions of particles in an equilibrium system. On short time scales, the particle would not yet have interacted with any other molecules or surrounding particles but over a longer period of observation these interactions affect diffusion. Surface forces and interactions are not negligible in some systems and the surrounding particles or gel network influence diffusion significantly. In this case, given that the diffusant molecule is large compared to voids in the system it may be trapped. The displacement of the diffusant depends on strength of interactions. The type of diffusant is also an important factor: Size, shape, flexibility and other properties like hydrophilicity and electrostatic interactions [4, 5].

2.1.2 Brownian motion and Einstein's relation

In 1827, Robert Brown, Scottish botanist discovered the random walk of suspended particles in fluid [5]. He noticed that this motion was general for organic and inorganic substances and different fine powders. This motion in honor of Brown, has been called "*Brownian Motion*"

A century later, Albert Einstein mathematically derived Brownian motion. Einstein was the first to understand that mean square displacement in a given time is a meaningful quantity instead of velocity [3]:

After Einstein, in 1913 Jean Perrin succeeded to relate component of the displacement X with gas constant (R), N Avogadro's number, η the medium viscosity ρ and the particle diameter. This relations is Einstein's relation with Stokes law for the viscous liquid medium [6]:

2.2. Soft matter systems

It can be seen that liquid or gas deforms in a continuous manner under the effect of a very slight external force, while most solids do not. But there are another state in many materials that are neither solids, nor simple liquids - they are somewhere in between. Soft matters are fascinating systems and are encountered in many everyday situations. Some examples of soft matter are paints, gels, plastics, liquid crystals and most of our body and food materials [7-9].

2.2.1. Permeability in different soft materials

The small structures inside all materials including soft materials, significantly affect their properties. For example, rheological properties (like Young's modulus) of a gel often depend on its microstructure. Diffusion or fluid flow inside a soft matter system also highly depends on its structure. Different gel structures might result in different permeability and mass flow properties and correlating permeability with these different structures would be fruitful and interesting in the field of soft materials. in a predictive way [10]. Mass transfer through composite materials like particle gel depends on the structure aggregation and network. Particle shape and particle volume fraction also are of importance. One may expect that diffusion through a material consisting of spheres vary linearly with the volume content of particles, However, E.L Cussler et al. investigated the impact of shape of particles on permeability of materials, as illustrated in Figure 1 [11]. Hence permeability in a composite material depends on the shape of particles as well as volume fraction of particles. Flakes are the geometrical shapes that result in the lowest permeability included in a composite.

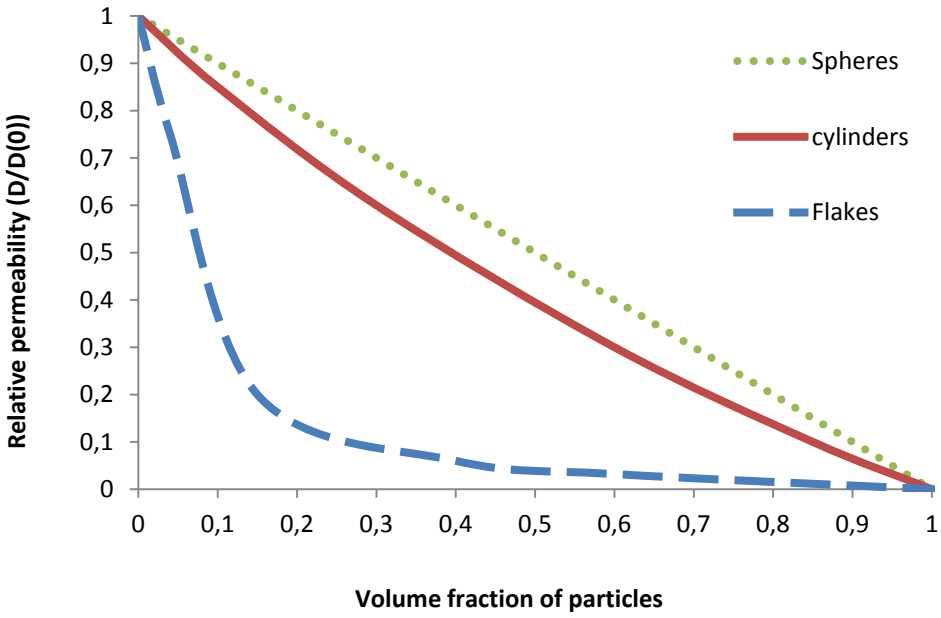

Figure 1 Permeability (through a composite material) versus volume fraction of different particle shapes. Flakes are aligned with aspect ratio 30 which has a significant difference with spheres (aspect ratio 1) and cylinders (aspect ratio 30)

2.3. Silica

Silica is the name for the oxides of silicon with the chemical formula, SiO_2. In nature it can be found in many states. Among them the crystalline state (like quartz sand)that is the most common state [12]. Silica sometimes is written as $[SiO_4]^{4-}$. This molecule has a tetrahedral shape and silica particles have negative charges on its surface. Silica can be synthesized and it can be either amorphous or crystalline. Crystalline silica like quartz has higher density (around 2.6 gr/cm^3) comparing to amorphous with density around 1.41 gr/cm^3 [13]. There is a similarity between water molecule and silica molecules. In silica, each silicon atoms is surrounded by oxygen atoms and in water oxygen atoms surround hydrogen atoms with slightly more open packing. Silica is somewhat soluble in water and hydrolysis of silica in water happens according to the equation:

$$SiO_2 + 2\ H_2O \rightarrow Si\ (OH)_4$$

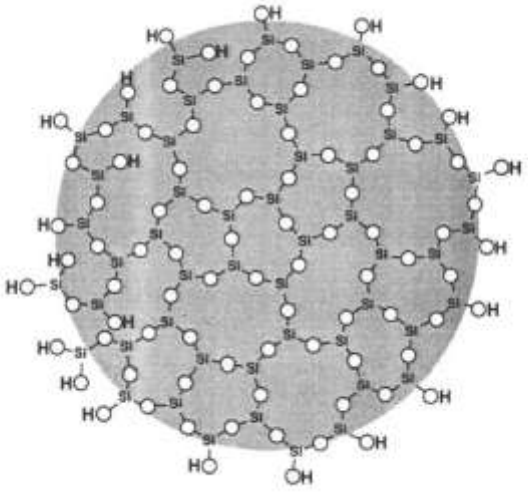

Figure 2 Schematic of hydroxylated colloidal silica particle in two dimensions. The fourth oxygen coordinated with Si is above or below the plane of the paper.(With permission from ACS, ref [10]. copyright 1994.)

2.3.1. Colloidal Silica

In general colloidal silica is a system in which finely divided particles with approximate particle sizes between 10 to 10,000 angstroms (Figure 2), are dispersed within a continuous medium in a manner that prevents them from being filtered easily or settled rapidly. To achieve such stability, these particles should be small enough for gravity to not to sediment the particles. In some application like membrane or separation, it is preferable if the size is large enough to prevent passing through a membrane while other molecules, ions and particles pass through the membrane. Colloids are systems with particles dispersed in a solvent (water in aqueous system is the most common) with a maximum size of 1 µm (1000 nm) and it is according to suggestion of International Union for Pure and Applies Chemistry (IUPAC) [14]. In Colloidal silica sols silica particles are dispersed in water solution has low viscosity depending on the grades from the manufacturing company. The range of sizes goes from about 1nm up to about 10µm [15]. Particle size distribution highly depends on the process in which they were created. The available silica concentrations are also limited and depend on factors that control the colloidal stability. [12]. Colloidal silica has a large surface area which depends on the size of particles but over particle size of 1 µm, the gravitational forces will be influential and colloidal system will be unstable unless applying other surface techniques like surface functionalization such as using extra charged particles in the continuous phase to resist the gravity forces of the big particles [10, 12, 15, 16]

2.3.2. Charged surface

The surface of colloidal silica is covered with hydroxyl groups with the formula of Si-O-H (Figure 3). These groups tend to dissociate in the aqueous solutions, yielding a high negative charge on the surface of each particle. Beside these hydroxyl groups sometimes and somewhere other groups have also been recognized including -Si-$(OH)_2$ or -Si-$(OH)_3$ or surface siloxanes, -Si-O-Si-O.

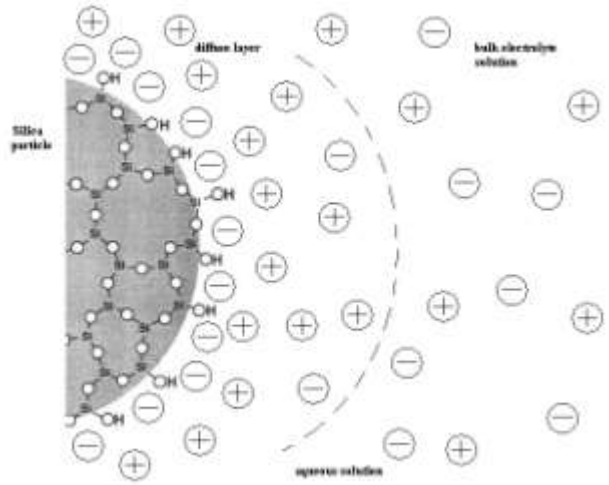

Figure 3 Double diffuse electrical layer s in aqueous solutions next to a silica particle.(Reproduced with permission from ACS, ref [10]. copyright 1994.)

The stability of colloidal silica depends to a large extent on the quantity of these charges and generally more negative charges make the system more stable. pH and the amount of electrolyte present are key factors for colloidal stability. Size of particles, silica concentration and storage temperature are other important factors [12].

2.4. Ostwald ripening

As mentioned previously, the size of particles is an important factor in dispersion or stability of colloids and colloidal silica sols as well. In all systems with small particle dispersions, there is Ostwald ripening phenomenon. According to IUPAC definition [14] “Ostwald ripening is dissolution of small crystals or sol particles and the redeposition of the dissolved species on the surfaces of larger crystals or sol particles. This process occurs because smaller particles have a higher surface energy, hence higher total Gibbs energy, than larger particles, giving rise to an apparent higher solubility” [12].

2.5. DLVO theory

An important theory for understanding particle-particle interactions and investigating colloidal suspensions is Derjaguin-Landau-Verwey-Overbeek (DLVO) theory. DLVO theory provides a framework to understand interparticle attraction forces (van der Waals dispersion) and repulsive forces (electrostatic interactions) together. This theory is the sum of those two potentials between two particles as described below [17-19].

The van der Waals forces between two particles with the same radius with center-to-center separation r is given by

Where is the Hamaker coefficient and depends on different factors like Boltzmann constant, absolute temperature, dielectric constant and refractive index of the particle and continuous phases.

The potential energy of repulsion between particles would be:

Where the vacuum permittivity, z is is the valence number of the ion, e is the charge of each electron, is the potential at the interface which with an approximation is zeta potential and is Debye length [17].

2.6. Colloid instability and Gelation

The stability of colloidal particles depends on surface-chemical modification of particles to provide either electrostatic and/or steric free energy barriers to aggregation [20]. When there are strong attractive interactions between colloidal particles, they might start to aggregate, sometimes phase separation occurs, and sometimes a gel forms [21]. On definition a *gel* is a "system made of a continuous solid skeleton made of colloidal particles or polymers enclosing a continuous liquid phase" [10]. Simply a gel consists of a solid network surrounded by a continuous liquid phase [22]. In colloidal silica sol systems, silica particles that overcome repulsive forces can link together and

form chains or three-dimensional network. This new state of material is a gel and it can be considered to have an infinite viscosity[16].

Gelation generally is termination of aggregation. A gel structurally is characterized by the formation of a macroscopic, space-filling particle/cluster network. At the gel point, large scale particle motion becomes strongly suppressed and structure formation is often irreversible [20]. In silica systems maximum stability of the sol is in general in a region around pH 8 and upwards and minimum stability with rapid gelation is found around pH 6. By adding NaCl in the system, the colloidal stability will be further decreased (Figure 4 and Figure 5).

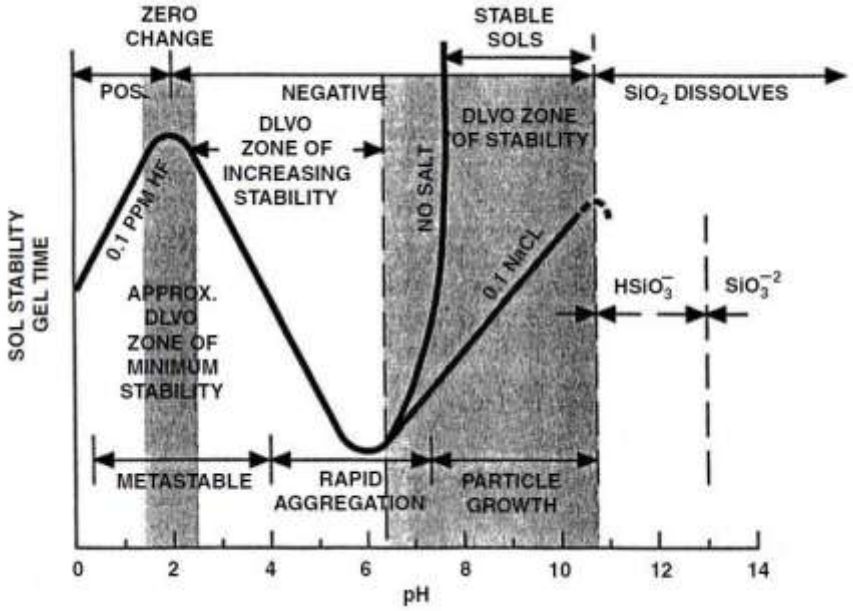

Figure 4 Effect of pH on the gelation and stability of colloidal silica. (With permission from John Wiley & Sons, Inc. ref [10, 16]. Copyright 1979.)

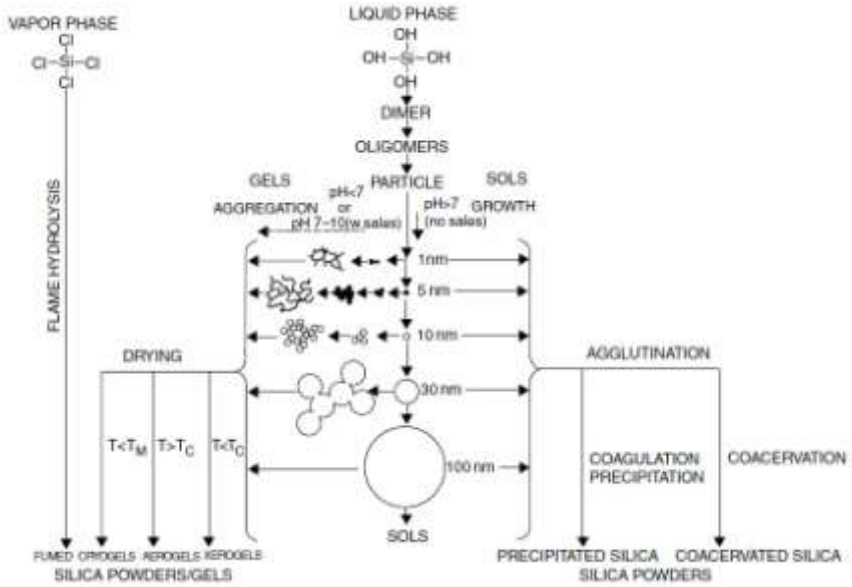

Figure 5 A genealogical tree of colloidal silica and polymerization behavior. Particles in sols grow in size with decrease in numbers: in acid solution or in presence of salts. In acid or pH 7-10 particles polymerize and create different type of gels bye different form of aggregation. (With permission from John Wiley & Sons, Inc. ref [10, 16]. Copyright 1979.)

2.7. Coagulation and Flocculation

There is a difference between gelation and coagulation or flocculation. Commonly the terms flocculation and coagulation are used interchangeably. Coagulation and gelation involves particles or molecules linking together and forming a 3D network. Coagulation or flocculation is precipitation of particles. The output of this process is two separated phases. In some cases this is hard to observe as separation due to high volume and low density of precipitate phase. The difference between coagulation and gelation is schematically is illustrated in Figure 6. Flocculation is a common in industry, for example in the flocculation of minerals like silica particles from water in mineral processing [10].

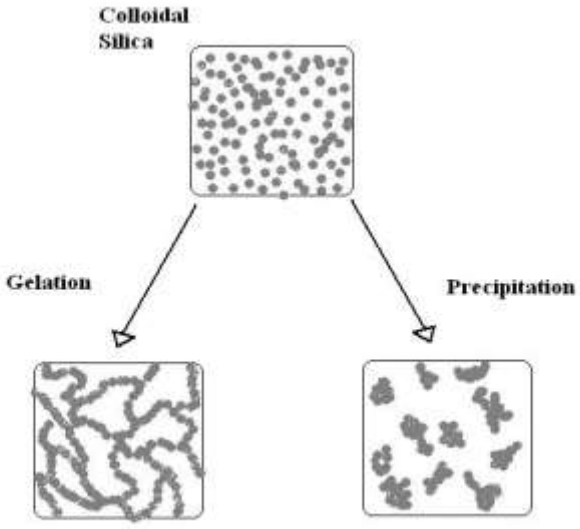

Figure 6 Difference between gelation and precipitation mechanism

2.8. Cellulose

Cellulose is a natural polymer found in nature. Wood, paper, and cotton all contain cellulose fiber. Cellulose is interesting because there is a global interest to shift to renewable material from ordinary plastic materials which is produced from fossil fuel. The main cellulose source in nature is wood which is a renewable source compared to synthetic polymers synthesized from fossil fuels. Cellulose is an environmentally friendly polymer which acts as a skeleton for the plants and wood. Cellulose has no taste, is odorless, hydrophilic and partially soluble in water and is biodegradable material.

Chain structure of cellulose contains repeated blocks of D-glucose with formula $C_6H_{10}O_5$ [23]. The chains of cellulose polymer are relatively stiff and have linear and functionalized structure. Nano cellulose consists of small cellulose crystals that have unique properties with growing application in different composite materials due to its anisotropic shape, dispersibility making it suitable as a reinforcing agent [25].

2.9. 1H NMR - Nuclear Magnetic Resonance

In this project NMR was used to study diffusion of water in silica particle gels. Diffusion NMR spectroscopy provides information about certain atoms in the bulk and is a powerful choice for measuring diffusion coefficients in multi-component systems. Diffusion coefficient reflects the

effective size and shape of a molecular species or particle as well as how the substance is interacting with its surroundings [24].

Conceptually there are two methods for measuring diffusion with NMR, Translational Diffusion in *Isotropic Systems—"Free Diffusion"* and the other method is *Restricted and Anisotropic Diffusion*. Two advantages of NMR method compared to traditional methods for measuring self-diffusion coefficients such as with radioactive tracers, are its simplicity and accuracy. 1H NMR allows simultaneous determination of diffusion coefficients in complex matters like gels [24].

2.10. QCM - Quartz Microbalance Crystals

QCM method was performed also to understand adsorption properties of silica/NCC particles in nano-scale with nano-gram accuracy. The quartz crystal microbalance (QCM) is a relatively new approach for measuring the mass of adsorption and desorption on different material surfaces. It is a real-time method for monitoring changes in the surface and interactions accurately. In this method the target surface should be covered on a quartz crystal in advance. Mass changes on the surface would be measured indirectly with the monitoring of changes in the frequency of the quartz crystal resonator. The resonance is disrupted by the addition or removal of a small mass due to changes in the thickness of the film. QCM method first used by William H. King and was able to demonstrate the capacity of quartz crystals for gas sorption detection [28]. The property of certain materials such as quartz pieosoelectric can be used as a tool for measuring the adsorption, the interaction between different particles and molecules. It could be used to measure the interactions between bio-interfaces in different environments or in a colloidal solution nano-cellulose/silica specifically. If the frequency measurement is made specifically, the frequency changes illustrate the thickness and mass on the surface with some relationships and modeling. In addition, the dissipation or damping is also measured with a QCM instrument to assist in the analysis and cross-check the results as well. With the measure of the trend of damping, viscoelastic characterization of this specific material would be feasible (Figure 7).

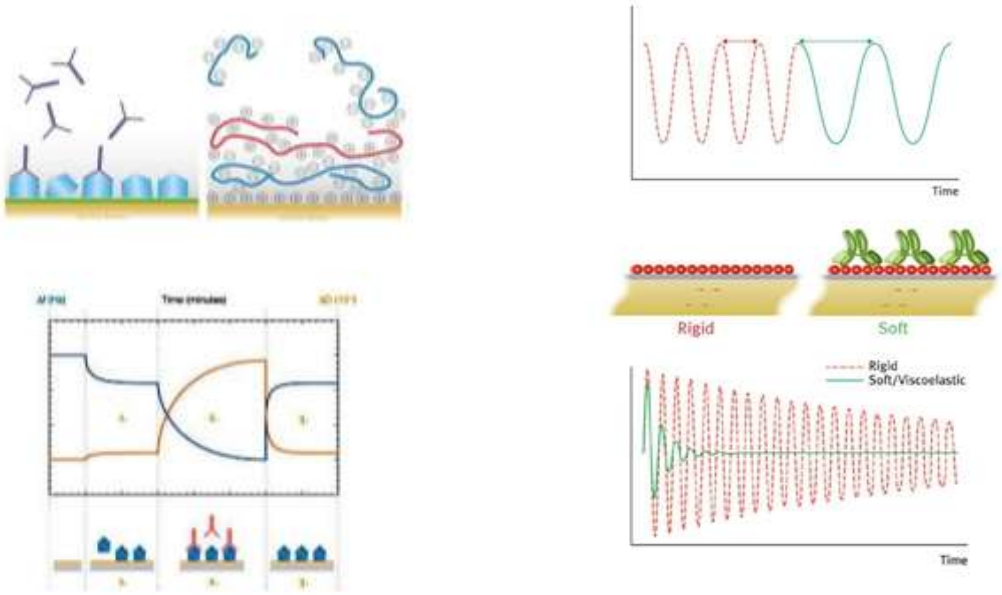

Figure 7 Left-up illustrate adsorption of 2 different molecules with two different mechanisms on prepared surface. Left-bottom shows frequency and dissipation during 4 different periods of adsorption and desorption which a raw data plot could look like. Right-up illustrates a change in frequency due to softening the film because of viscoelastic properties of the new (green) layer. And left bottom shows dissipation in a rigid film (red) comparing with a new film which is softer.(with permission from Q-sense Company, ref. [25])

2.11. TEM - Transmission Electron Microscopy

In TEM, a beam of electrons is transmitted through a very thin layer of a hard specimen. Emitted electrons will have an interaction influencing by size, shape and physics of the specimen and these differences in interaction provide a contrast in the image. In other words output of TEM is a 2D projection of a thin 3D object. In this project, TEM was used to investigate the nano/micro structure of the generated materials.

2.12. Purpose

The long term purpose is to be able to do predictive design of mass transport properties by controlling micro/nano-structure in the different soft composite systems. This knowledge is to be used by, for example the *SuMo* partners to construct better products.

2.13. Aim

The aim is to create a model material for studies of mass transport in nano and micro porous materials, more specifically this work will focus on creating a library of different structures to be studied and to characterize the structure and diffusion properties of these materials.

Chapter 3 Methods

Different pseudo-phase diagrams were done at four different pHs. This was done in 800 µl test tubes were the liquid/gel volume was 300 µl. This part of the studies aimed at mapping out which silica and salt concentrations that resulted in gels that was mechanically stable enough to go through the process of embedding (before cutting and imaging in TEM). These studies also aimed at gaining an over understanding of aggregation processes taking place in an destabilized sol

3.1. Materials

- The colloidal silica used was BINDZIL 40/130 from Eka Chemicals Company, Sweden with 40 weight% silica. pH of the stock colloidal silica was in the range of 9.10-9.30.

3.1.1. Nano-cellulose preparation:

- Nano-cellulose prepared according to a protocol in a published article in 2008 by Merima Hasani, et al. [26]. Cellulose was hydrolysed by Sulphuric acid (64% w/w, Sigma at 45 °C for 45 minutes. Typically, 10 g of cotton filter aid was treated with 175 ml of acid. Immediately following the acid hydrolysis, the suspension was diluted 10-fold with MilliQ to quench the reaction. The suspension was centrifuged and re-suspended repeatedly to remove excess water and acid. The suspension was then dialyzed until constant neutral pH was achieved in the effluent and there were no change in conductivity. To concentrate the NCC, rotoevaporation was used. The suspension was then sonicated (Vibracell Sonicator, Sonics and Materials Inc., Danbury, CT) while cooling in an ice bath, Mixed-bed research grade ion exchange resin (DOWEX MR-3 from Sigma) was added to the cellulose suspension for 48 hours, and then removed by filtration through hardened ashless filter paper Whatman 541 (pore size 22µm). The nanocrystals were then converted from the protonated sulphate ester to the sodium salt by conductometric titration with 0.0020 M NaOH.

3.1.2. Sample preparation for phase diagrams

Samples are prepared by varying silica, nano-cellulose (NCC) and NaCl concentrations and phase behavior was monitored at different time points. The vessel (chosen for this purpose was small and transparent glass tubes with about 800 µl total volume, AR-Sodaglas (6×35mm). Geometry of tubes was similar to NMR tubes but shorter in length (Figure 8).

The measurements of pH were done with a pH meter, model 744 from Ω Metrohm. Protocol of pH adjustment of silica sols will be discussed later in detail.

In order to yield reproducible results pH adjusted silica was added to the tubes after salt solution and milliQ had been added. When NCC was added to the system the procedure was the same, except that NCC was added before silica solution.

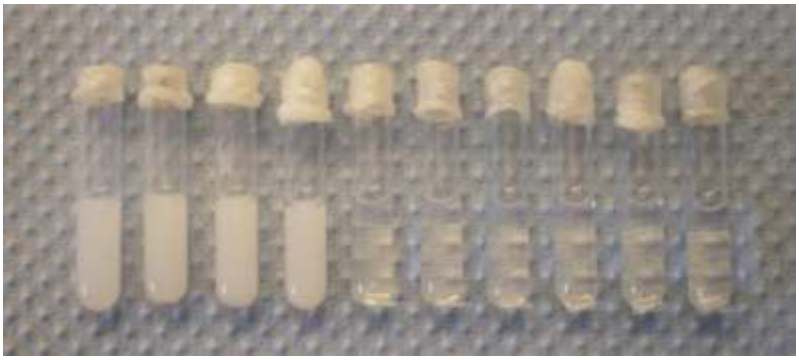

Figure 8 10 glass tubes witch containing constant silica with different salt content from 0.9 M in the left to 0.01 M in the right

After these steps, the tubes were left standing in an upright postion and data was recorded after roughy 1, 3, 13, 20 and after 60 days depening on the experiment series. Things that were noted in the tubes was if it had gelled, if it was phase separated and in that case the relative amount of lower phase was recorded.

3.1.3. Protocol for adjustment pH at 7.8

1.5 g of ion exchanger (Dowex Marathon MR-3) was added to a small beaker and mixed with a magnetic stirrer. For 40% SiO_2 solution the ion exchanger was filtered after around 90 seconds at pH 8.60 and for 10% SiO_2 solution after around 1 minute at pH 7.9. Filtration was done with a vacuum Erlenmeyer. pH was measured after filtration resulting in a final pH of around 7.8

3.1.4. Protocol for adjustment pH at 6

The ion exchanger (Dowex Marathon C) was firstly washed to remove excess acid from the surface of ion exchanger. 0.7 g of ion exchanger was added onto the filter paper and washed with around 40 ml of MilliQ, then filtered dry with suction filtration. The ion exchanger was then added to the silica dispersion and mixed with a magnetic stirrer. The ion exchanger was filtered of with suction filtration after 3-4 minutes for 40% SiO_2 at pH 5.9 and for 10% SiO_2 solution at pH 6. The pHs of the solutions were close to pH 6 after filtration.

3.1.5. Protocol for adjustment at pH 4

The protocol for this pH adjustment was similar to the adjustment at pH 6 except that the ion exchanger was filtered of after 4-5 minutes for 40% SiO_2 solution at pH 3.9 and for 10% SiO_2 solution at pH 4.0 The pHs of the solutions after filtrations were close to pH 4.

10 samples of these tubes can be seen in Figure 8 which all mixtures are prepared after compounding with above procedure.

3.2. Inverted tube method

Monitoring of gelation and observation of tubes (containing sols or/and gels) has been done by visual checking and by applying stress by inverting and gently shaking each tube by hand. This method is called the "inverted tube method" and this method is a criterion to determine when the particle network is spanned the entire system and a mechanically stable gel is created.

Accordingly, if the liquid in the tube was flowing without any shaking, it was classified as a "*solution"* and called a "*sol*". In the case of a slow viscous flow similar to a viscous oil or molten glass for instance, it was defined as "viscous". If it did not flow when inverted, but it did flow after gentle shaking, it was referred to as a "*semi-gel*" which is a mechanically unstable gel. "*Gel*" was defined as a gel when it did not flow when the tube was inverted and gently shaken. Finally, samples that sedimented or shrunk is shown in the phase diagrams with a cross. Sometimes the cross has percentage value next to it describing how many percentage of the total sample volume that was occupied by the lower sedimented phase.

3.3. 1H NMR diffusometry test

Diffusion measurements were carried out on a Bruker DMX600 spectrometer, equipped with a Bruker Diff30 probe of 1200 G/cm maximum gradient strength and with a 5 mm RF 1H coil. All diffusion experiments were performed with Δ=500 ms diffusion time, δ = 1 ms gradient pulse length, and the gradient strength linearly ramped in 17 steps from 0 to 30.03 G/cm in the conventional stimulated-echo sequence. Relaxation delay to thermal equilibrium, D1, was set to 15 s and each experiment encompassed a collection of 4 acquisitions. The size of tubes (containing sols or/and gels) in inverted tube method were chosen similar to standard NMR tube size (same diameter with the shorter length). It causes to keep the same geometrical condition for the gelation process inside the NMR tubes and inside the tubes for the phase behavior studies (tube size and the gelation procedures were described previously). NMR diffusometry was performed after 13 or 14 days after the preparation of the gels inside the NMR tubes (this time was chosen according to gelation times in those specific samples).

3.3. Embedding and TEM imaging

Firstly, gel samples was cut in 1×1×1mm size pieces and then dehydrated and fixed. The embedding makes it possible to investigate the gels by TEM and remedies the problems that could come from gel softness and presence of water. The fixation in a plastic, allow sectioning and microtome cutting of gels. The gels were exposed to increasing concentrations of ethanol after which they were put into solutions of resin in ethanol. Polymerization took place at 60 ºC and ultrathin sections (~60 nm) were cut with a diamond knife using an Ultratome Reichert-Jung Ultracut E (Reichert-Jung, Germany). The thin sections were placed on 400mesh cupper grids. The used TEM instrument was a model LEO 706E made in LEO Electron Microscopy Ltd., Cambridge, England. An accelerating voltage of 80 kV was used.

Chapter 4 Results

In section 1, pseudo-phase diagrams are presented for pure silica or NCC or a mixture them in different pHs and different ion strengths. The experiments were done to study the kinetics of aggregation and gelation for the different systems.

In section 2, the QCM measurements of colloidal silica and NCC interactions at varying pH and silica concentrations will be presented. Section 3 contains a SEM image showing NCC fibers dried onto a surface. In the next following section, section 4, TEM results are presented for different gels. Values of the diffusion coefficient in different gels are shown in section 5 derived with the 1H-NMR method.

4.1. Section 1- Pseudo-phase diagrams

Investigations were done to find out under which conditions (time, pH and silica/NCC concentrations) mechanically stable gels can form. Mechanically stable gels are needed for the microstructure not to break when cutting the gels into pieces before embedding. The resulting pseudo-phase diagrams varying these factors are presented below.

4.1.1. Section1-Part1 Varying concentration of silica and NaCl at pH 7.8

The range of silica content was from 1 to10 weight percent and the range of the NaCl concentration was 0.01 M to 0.9 M. After 3 weeks, phase separation started to show in the samples that contained relatievely low concentrations of silica and medium to high concentration of NaCl (Figure 9, Figure 10 and Figure 11). Gelation occurred at 0.3 M NaCl and above 4 wt% silica. Sedimentation develpoed in semi-gel samples and solution samples. Often when phase separation occurs the lower phase is not mechanically stable and the lower phase behaves like sand sedimented in water.

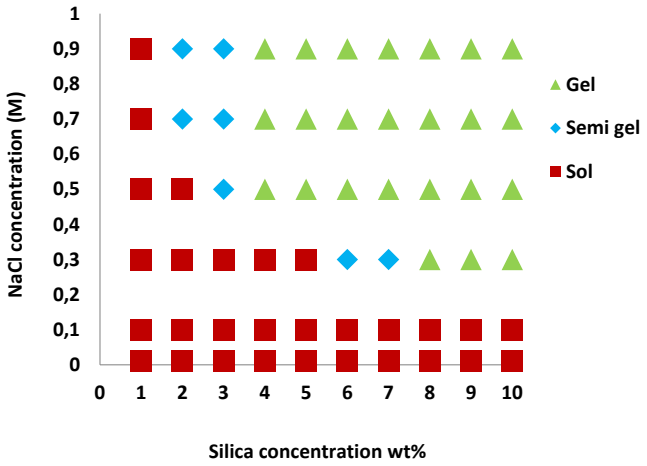

Figure 9 NaCl concentration versus colloidal silica concentration at pH 7.8, after 3 days.

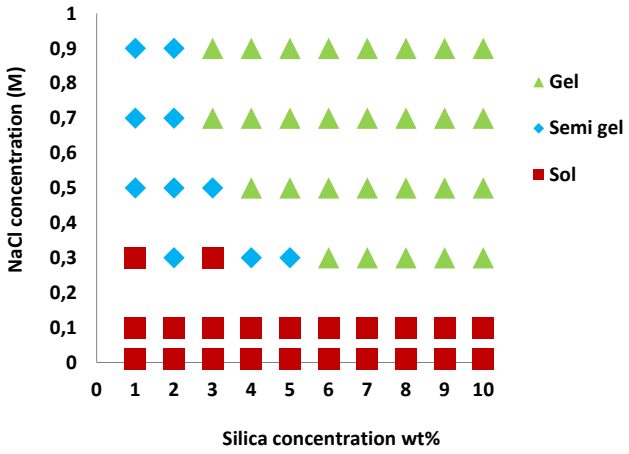

Figure 10 NaCl concentration versus colloidal silica concentration at pH 7.8, after 20 days.

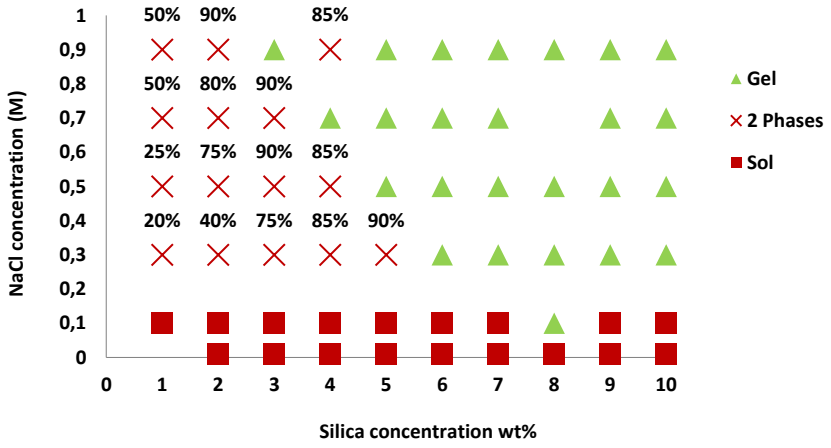

Figure 11 NaCl concentration versus colloidal silica concentration at pH 7.8, after 60 days. Sediment volume out of total sample volume is stated over each ssedimented sample (Missing sample pointswas due to died out sample because of inappropriate sealing with para-film)

Pseudo-phase diagram at pH 7.8

In Figure 12, the time dependence of gelation at pH 7.8 is illustrated. The gelled region grows up till days 20 and then shrinks up to 60 days.

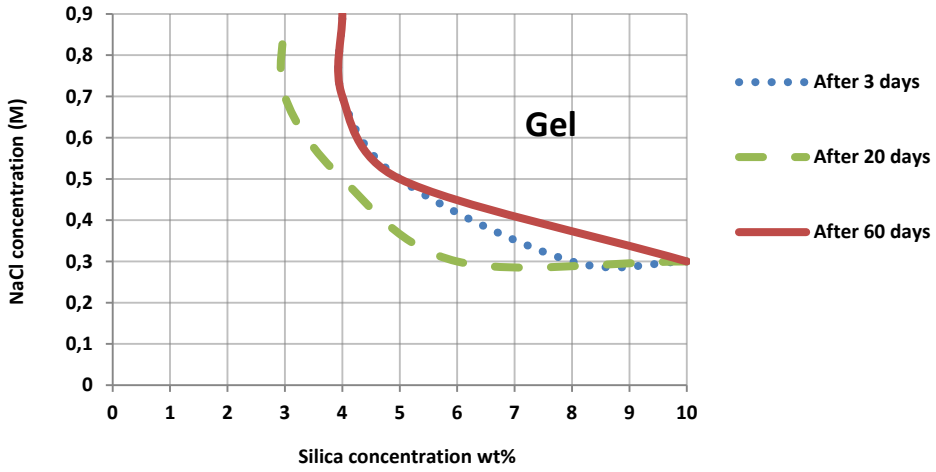

Figure 12 Pseudo-phase diagram of colloidal silica concentration versus NaCl concentration at pH 7.8, after 3 different time points. 0.3 M NaCl was the lower concentration needed for gelation at this pH. The corresponding silica concentration for gelation was 3 wt%.

.

4.1.2. Section 1-Part 2 Varying concentration of silica and NaCl at pH 6

In pH 6, five time points was recorded, 1, 3, 13, 45 and 60 days. These are illustrated in Figure 13-Figure 17.

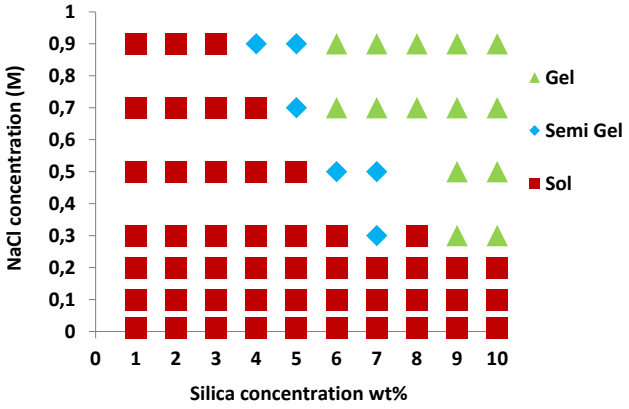

Figure 13 NaCl concentration versus colloidal silica concentration at pH 6, after 1 day.

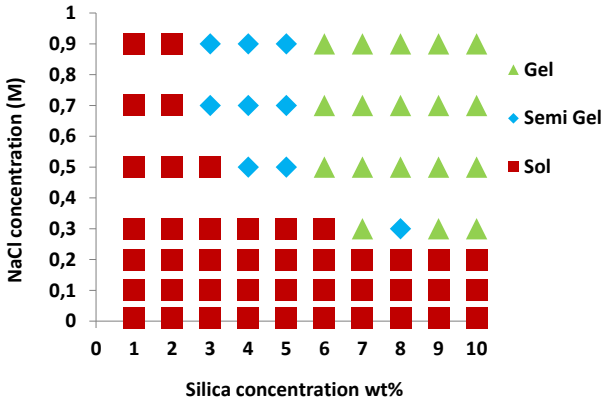

Figure 14 NaCl concentration versus colloidal silica concentration at pH 6, after 3 days.

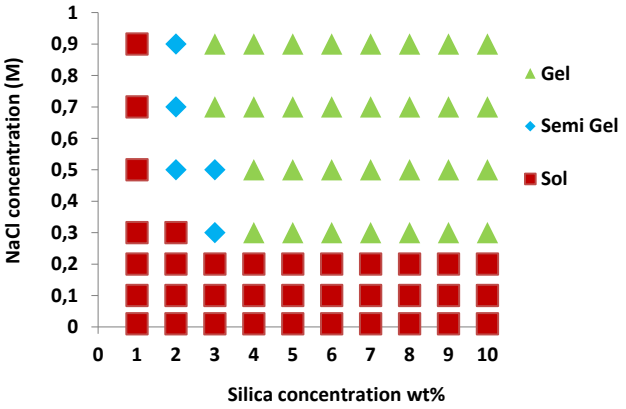

Figure 15 NaCl concentration versus colloidal silica concentration at pH 6, after 13 days. Gel area expanded to silica 3 wt% and above 0.3 M NaCl the samples gelled.

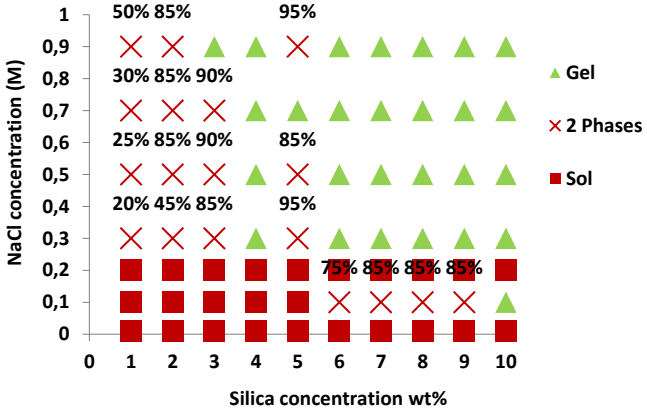

Figure 16 NaCl concentration versus colloidal silica concentration versus NaCl concentration at pH 6, after 45 days. Many samples with low silica content phase separated (cross points) .

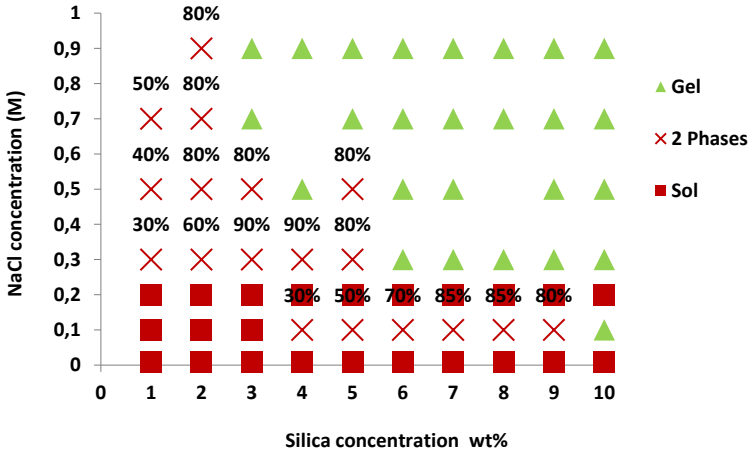

Figure 17 NaCl concentration versus colloidal silica concentration at pH 6, after 60 days. The phase behavior remained mostly stable between 45 and 60 days. (Missing points are samples which are dried due inappropriate sealing with para-film)

When the sol has been destabilized it starts to aggregate and sometimes gelling occurs in samples. At all time points at pH 7.8, gelation takes place above 0.3 M NaCl. At day one (Figure 13) the minimum silica concentration needed for gelation is 6 wt%. The gelation regime gradually expanded over time to the lower silica concentration and after 13 days (Figure 15) a maximum extent of the gelation region is reached, were gelled samples was found at as low concentration as 3 wt % silica.

At 45 days many samples transformed from one phase to two separated phases. This process started earlier, perhaps already after 2 weeks, however the recording of when samples had phase separated or did not start until 45 days, at which time it was deemed interesting to record. The thickness of the lower phase seems to become larger with increasing silica and NaCl concentration. Between 13 and 45 days the gel region shrunk but after that up to 60 days the gelled region did not change much (Figure 15-17).

Pseudo-phase diagram at pH 6

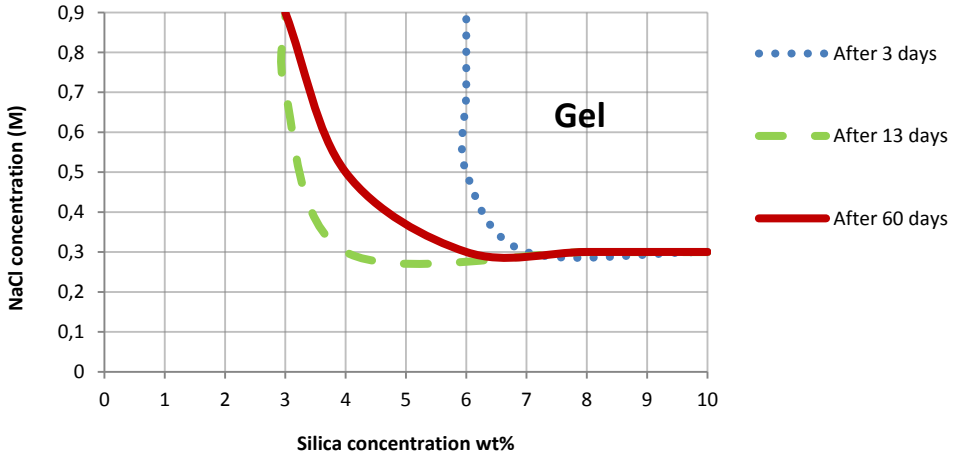

Figure 18 Pseudo-phase diagram of NaCl concentration versus colloidal silica concentration at pH 6, after 3 different time points. Gelation area grew up until day 13 and then shrunk. Boundary condition and minimum required ionic strength for gelation was 0.3 M NaCl and stable gels were formed in above 3.5 %wt of silica.

A few gelled samples from day 45 had phase separated at day 60.

4.1.3. Section 1- Part 3 Varying concentration of silica and NaCl at pH 4

In pH 4, three time points was recorded 13, 45 and 60 days. These are illustrated in Figure 19, Figure 20 and Figure 21

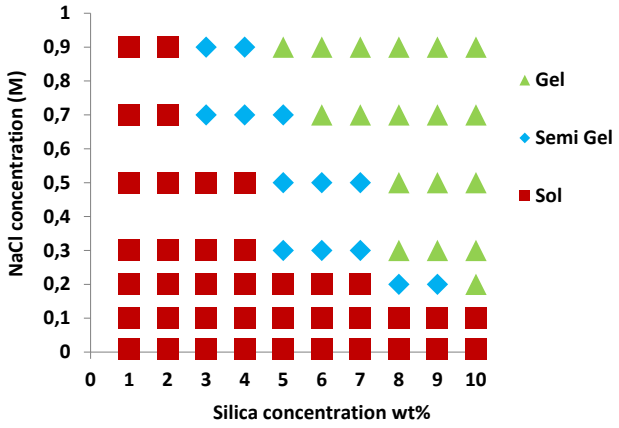

Figure 19 NaCl concentration versus colloidal silica concentration at pH 4, after 13 days

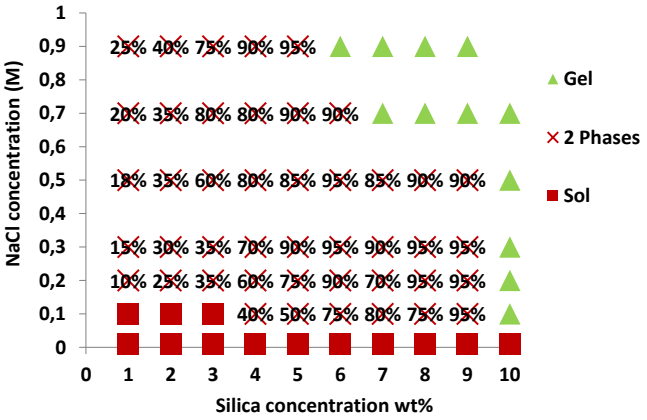

Figure 20 NaCl concentration versus colloidal silica concentration at pH 4, after 45 days. (Missing points are samples which dried out due to leaking sealing with para-film)

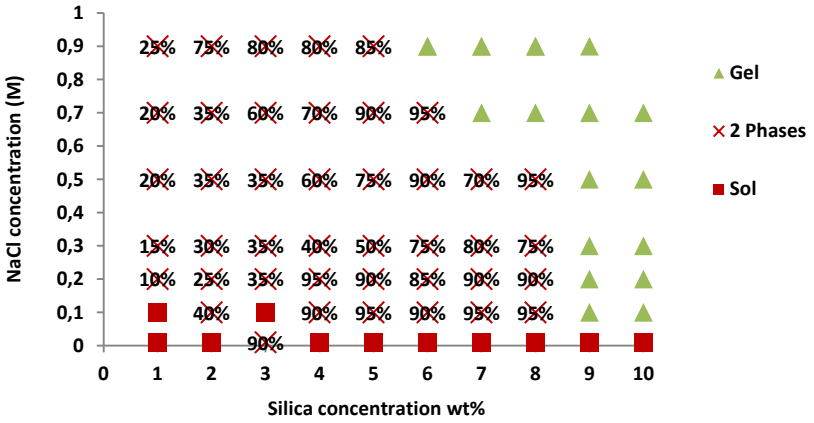

Figure 21 NaCl concentration versus colloidal silica concentration versus at pH 4, after 60 days.

Pseudo-phase diagram at pH 4

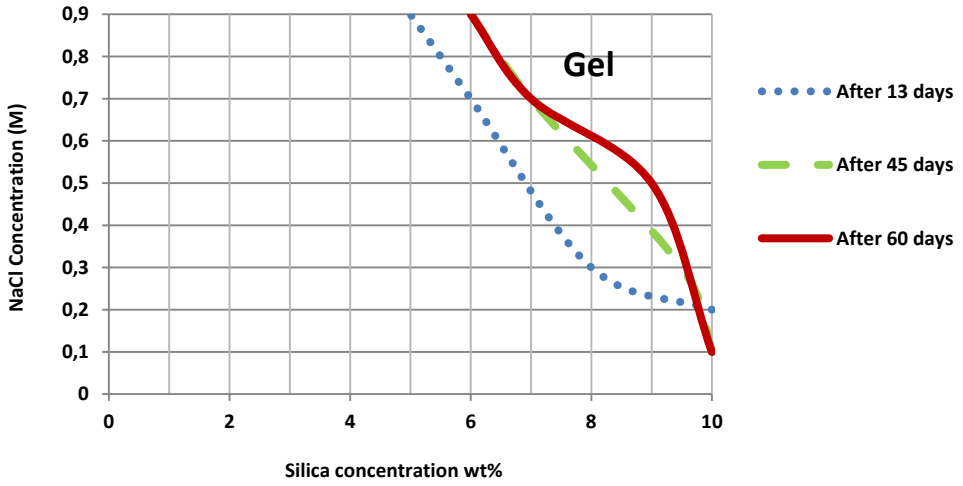

Figure 22 Pseudo-phase diagram at pH 4 at 3 different time points

The main difference in phase behavior at pH 4 was the kinetics of aggregation and gelation. In comparison with the similar systems at pH 6 and pH 7.8, there was a significant delay in gelation and the first gels appeared after around 10 days which was quite long time compared to higher pHs. The minimum silica concentration for gelation is around 5 wt% and minimum required ionic strength for gelation is 0.1 M NaCl (Figure 19-21). Overall the size of the gelled region is much smaller at pH 4 compared to pH 6 and 7.8.

Phase separation could clearly be seen at 45 days (Figure 20) and this zone was comparably larger in pH 4 (see Figure 21 and Figure 22 after 60 days). There were two types of phase separation, one resulting from shrinkage, leading to a mechanically stable lower phase, but also another process more similar to sedimentation where the lower phase was not mechanically stable when the tube was inverted.

4.1.4. Section 1-Part 4 Gelation of pure NCC in existence of constant NaCl after 1 day

In order to investigate the gel formation of NCC solutions containing only NCC was mixed with NaCl solution. The NCC solution without NaCl was slightly viscous compared to water already from the beginning, upon addition of NaCl the NCC dispersion became even more viscous reaching a semi-gel state. The viscous state that was recorded is illustrated in the phase diagram bellow (yellow circle points, Figure 23). In these points viscosity of solution increased and when tubes were inverted a flow occurred with a notable retardation in flow speed. The viscous state was a behavior intermediate between solution and semi-gel.

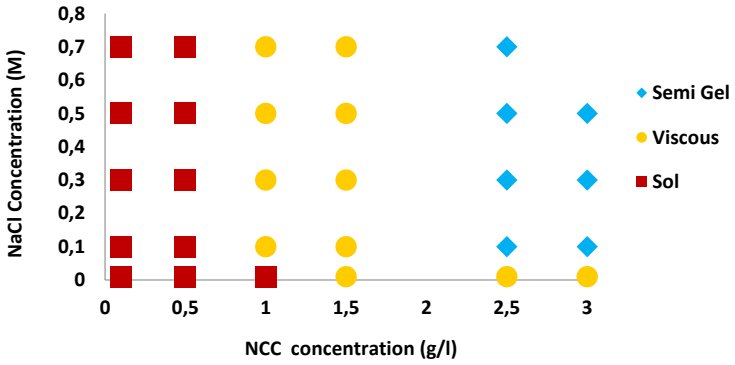

Figure 23 Effect of varying NaCl and NCC concentrations on gelation of pure NCC after one day

Minimum NCC content for semi-gel was around 2.5 g/l with minimum 0.1 M NaCl (Figure 23-24). In the range of 1-1.5 g/l NCC, most of the samples exhibited an increase in their viscosity (referred to as "viscous". Below 1 g/l NCC the viscosity remained unaltered compared to samples without added NaCl. As expected no changes in the phase behavior occurred over time and therefore only one time point is presented here.

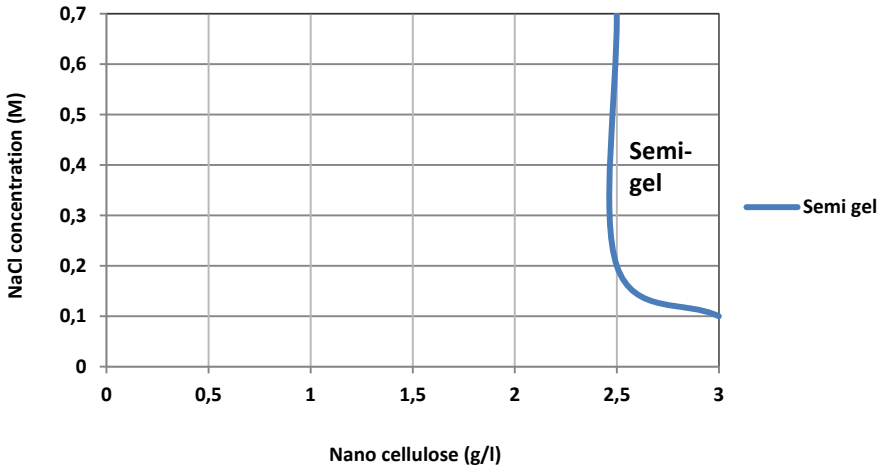

Figure 24 Pseudo-phase diagram of pure NCC

4.1.5. Section 1- Part 5 Effect of colloidal silica on Pseudo-phase behavior of NCC

During day two, silica at pH 7.8 was added to all NCC samples shown in Figure 25. The end concentration of silica was 5 wt%. Observation of the phase behavior was done at three time points and results are illustrated in Figure 25, Figure 26 and Figure 27.

After the silica was mixed in with the NCC dispersion, the phase behavior of new system exhibited a notable change. After one day (Figure 25) all samples with 0.6 M NaCl formed a gel.

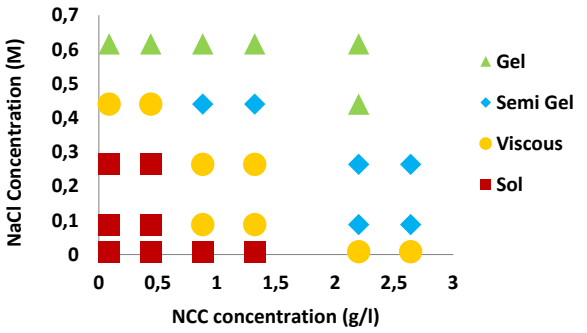

Figure 25 Pseudo-phase behavior of NCC mixed with silica at constant concentration (5 wt% silica) After 1 day (Missing points was samples which dried due to inappropriate sealing with para-film)

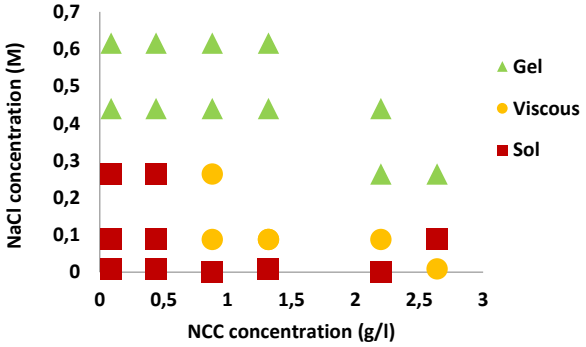

Figure 26 Pseudo-phase behavior of NCC mixed with silica at constant concentrations (5 wt% silica) after 3 days

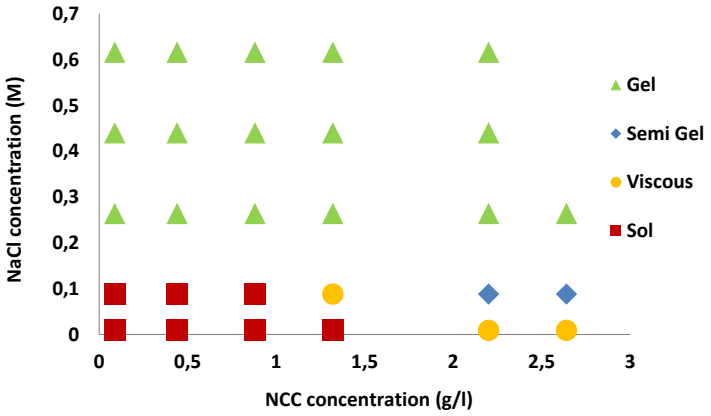

Figure 27 Pseudo-phase behavior of NCC in existence of constant silica concentration (5 wt% silica) after 30 days

After 3 days (Figure 26) all samples with 0.4 M NaCl and upwards had gelled. Reaching 30 days, samples seemed to be getting close to a steady-state condition were all samples with salt concentrations higher than 0.25 M had gelled. There was no phase separation (sedimentation) in any sample.

4.1.6. Section 1- Part 6 Pseudo-phasediagram of NCC/silica in constant NaCl concentration at pH 7.8

NCC, silica and NaCl solution was mixed and the phase behavior was observed at three different time points. The results are illustrated in Figure 28, Figure 29 and Figure 30.

Figure 28 Phase behavior of NCC and silica system with a constant NaCl concentration of 0.5 M NaCl. day 1 at pH 7.8

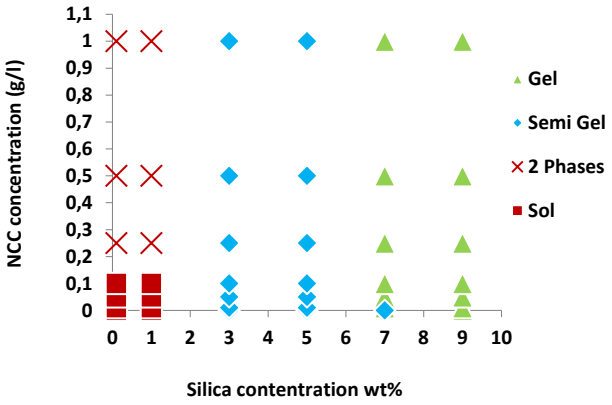

Figure 29 Phase behavior of NCC and silica system with constant NaCl concentration of 0.5 M ,day 3 at pH 7.8

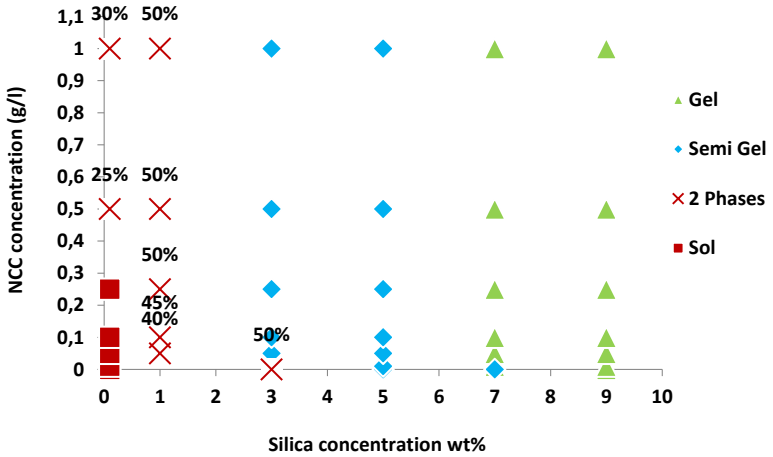

Figure 30 Phase behavior of NCC and silica system with constant NaCl concentration of 0.5 M ,day 27 at pH 7.8

The relative amounts of sedimentation are shown in Figure 30. In this test the effect of silica and NCC concentration was investigated. After one day as it is shown in Figure 28 all samples with 9

wt% silica gelled. An interesting observation found in Figure 28 was phase separation (sedimentation) from day 1. This process occurred at 0.2 g/l NCC or above otherwise, the samples remained in sol state (See crossed points in Figure 28 and Figure 29). This diagram shows that that silica concentration had the main role in determining the phase behavior (see phase behavior changes in different silica concentrations in Figure 28 to Figure 30). However, different concentration of NCC at low silica concentration did affect the sedimentation.

After 3 days, the gel region expanded to lower silica concentration and the minimum silica concentration for gelation was 7 wt%. Some sedimented samples turned into semi-gels, which might be because of re-mixing of the samples when inverting the tubes for observation. In Figure 30 the phase behavior after 27 days is illustrated. Gelling occurred at 7 wt% silica and above and biphasic samples were at 0.1 and 1 wt% silica. No significant change in the phase behavior was observed from day 3 to day 27 and some type of equilibrium state) seems to have been reached.

4.1.7. Section 1- Part 7 Pseudo-phasediagram of NCC/silica in constant NaCl concentration at pH 9.25

In this test the NCC/silica phase behavior at pH 9.25 was investigated. The silica solution used in these samples was the original solution without ion exchange treatment to lower the pH. The overall behavior here was similar to the phase behavior observed at pH 7.8 except that the gel region was slightly larger. After the first day almost all samples with silica concentration higher than 5 wt% became to gels (Figure 31). Figure 32(day 3), Figure 33(day 13), Figure 34(day 20) and Figure 35(day 27) show the comparison between volume fraction of sedimented phase in each point in different time. These percentages slightly increased by time in some samples but the general phase behavior remained the same. The phase behavior remains roughly unchanged at 3 days except a few solutions that had turned viscous.

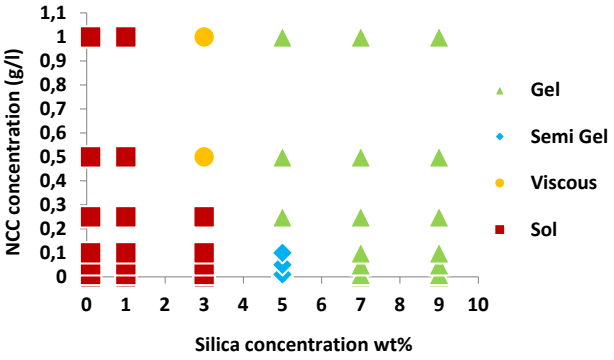

Figure 31 Phase behavior of NCC and silica system with constant NaCl concentration of 0.5 M NaCl after 1 day in pH 9.25

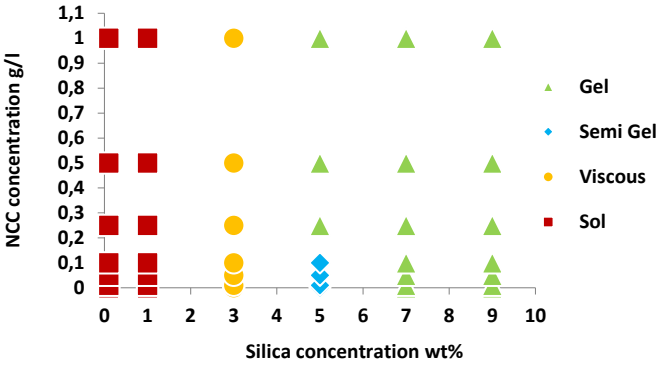

Figure 32 Phase behavior of NCC and silica system with constant NaCl concentration of 0.5 M NaCl after 3 days in pH 9.25

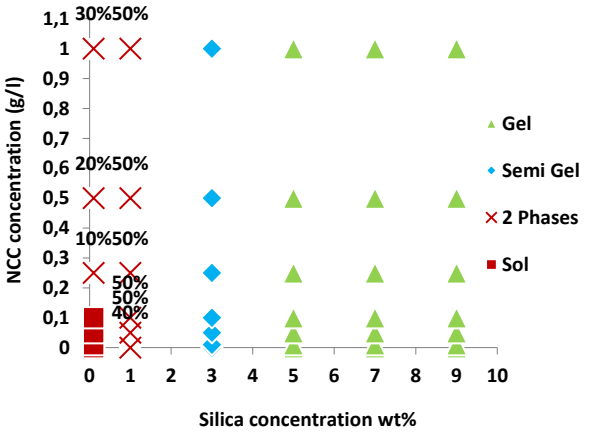

Figure 33 Phase behavior of NCC and silica system with constant NaCl concentration of 0.5 M NaCl after 13 days in pH 9.25

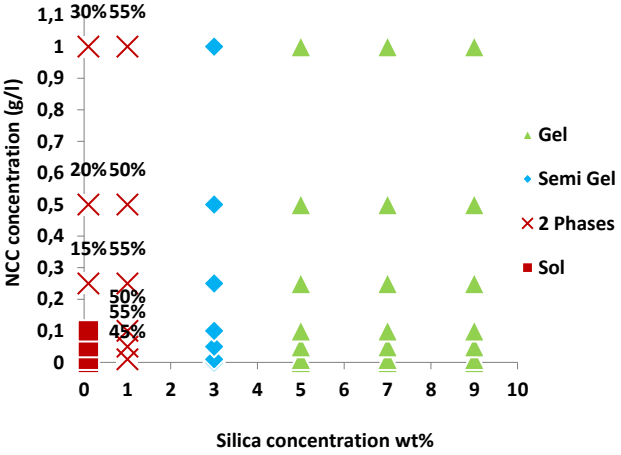

Figure 34 Phase behavior of NCC and silica system with constant NaCl concentration of 0.5 M NaCl after 20 days in pH 9.25

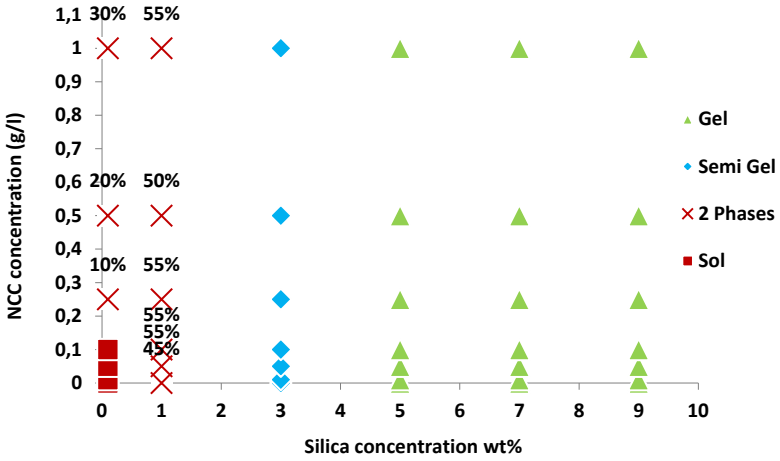

Figure 35 Phase behavior of NCC and silica system with constant NaCl concentration of 0.5 M NaCl after 27 days in pH 9.25

4.2. Section 2-Mass adsorption results with QCM-D method

4.2.1. Section 2-Part 1 Effects of Silica concentration on APTMS surface at constant pH 2.0

QCM-D was used to probe the interaction between silica and nano cellulose. Such measurement was to increase the understanding of how silica and nano cellulose would interact with each other after destabilization at different pHs in the sol, and in the silica gels. A model surface of NCC was therefore spin coated onto pretreated QCM-D crystals, creating a film on NCC. The surface was then exposed to flow of a sol of low concentration colloid silica at different pHs and constant NaCl concentration under flow.

In order to find which concentration of colloidal silica that was needed for saturation of the QCM-D crystal, an APTMS surface was exposed to three different concentrations of colloidal silica. This experiment in some ways acts as a control for experiments described further down were the APTMS is covered with NCC. The results from the QCM-D measurements of silica adsorption onto APTMS surfaces are shown in Figure 36-Figure 38.

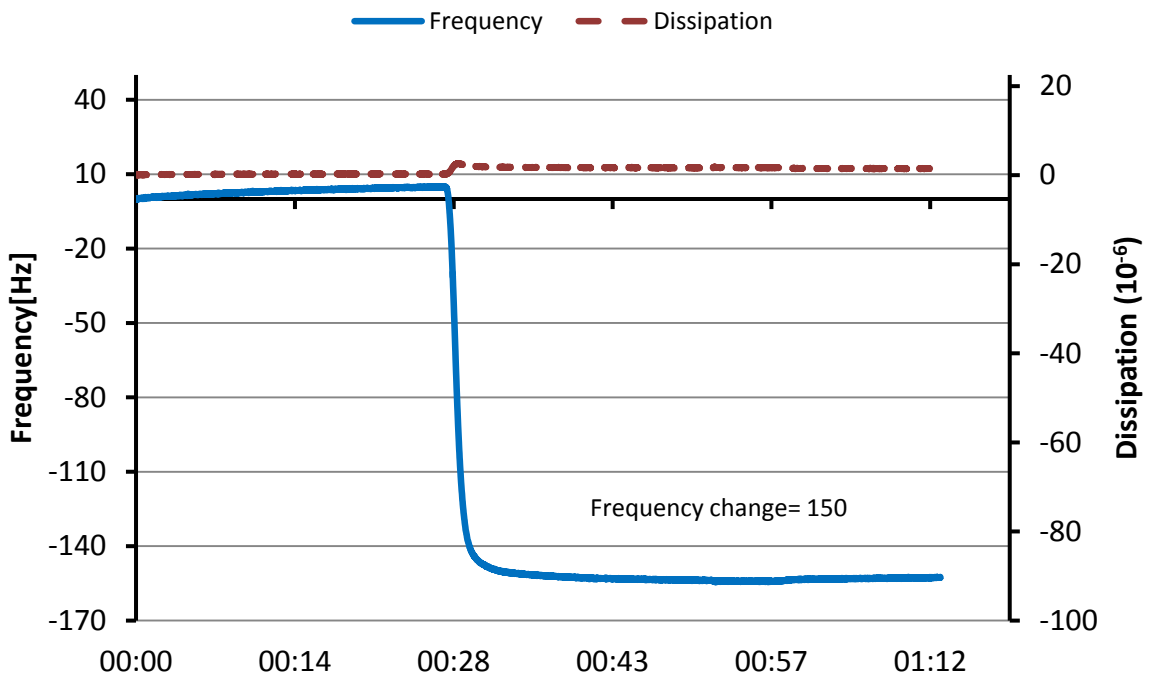

Figure 36 Silica adsorption on APTMS surface in low silica concentration (0.004 wt%). Approximate frequency change is 150. The graph is based on the third overtone.

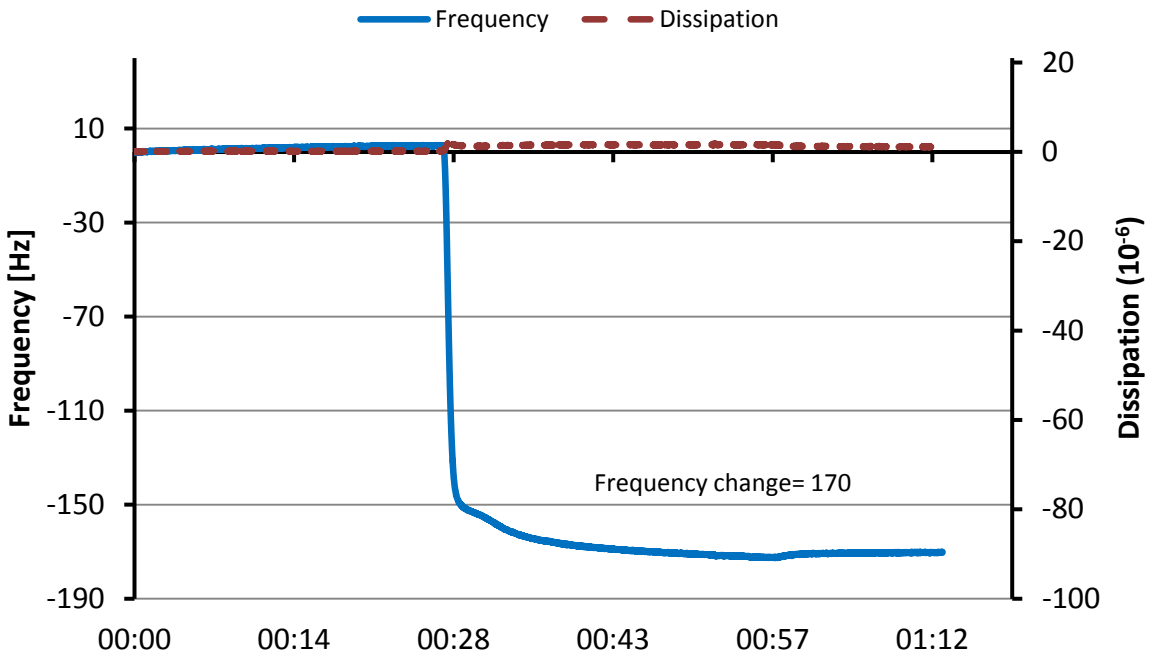

Figure 37 Silica adsorption on APTMS surface in medium silica concentration (0.04 wt%). Approximate frequency change is 170. The graph is based on the third overtone.

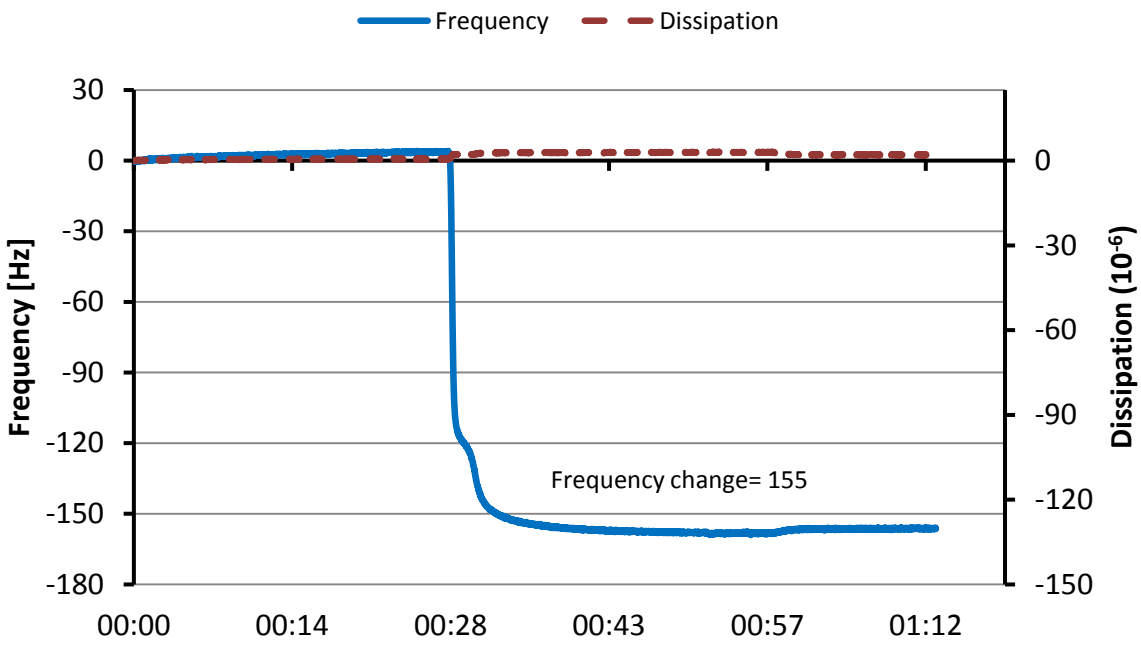

Figure 38 Silica adsorption on APTMS surface in higher silica concentration (0.4 wt%). Approximate frequency change is 155. The graph is based on the third overtone.

In this test increasing silica concentration from 0.004 wt% to 0.04 wt% firstly increased frequency approximately from 150 to 170 but increasing silica concentration to 0.4 wt% decreased frequency again to around 150. Overall change of frequency was not significant. It seems that the amount of adsorption of silica particles on to the APTMS surface was the same independently of the silica concentration used.

4.2.2. Section 2-Part 2 Effects of Silica concentration on NCC surface at constant pH 2.0

In this experiment the goal was to look at the interaction between NCC fibers and silica particles in three different concentrations of silica solutions. This is the continuation of the previous experiment were in Figure 36-38 and a comparison of the frequency changes are illustrated which each frequency can represent a specific thickness of silica on the surface of NCC (Figure 39-41).

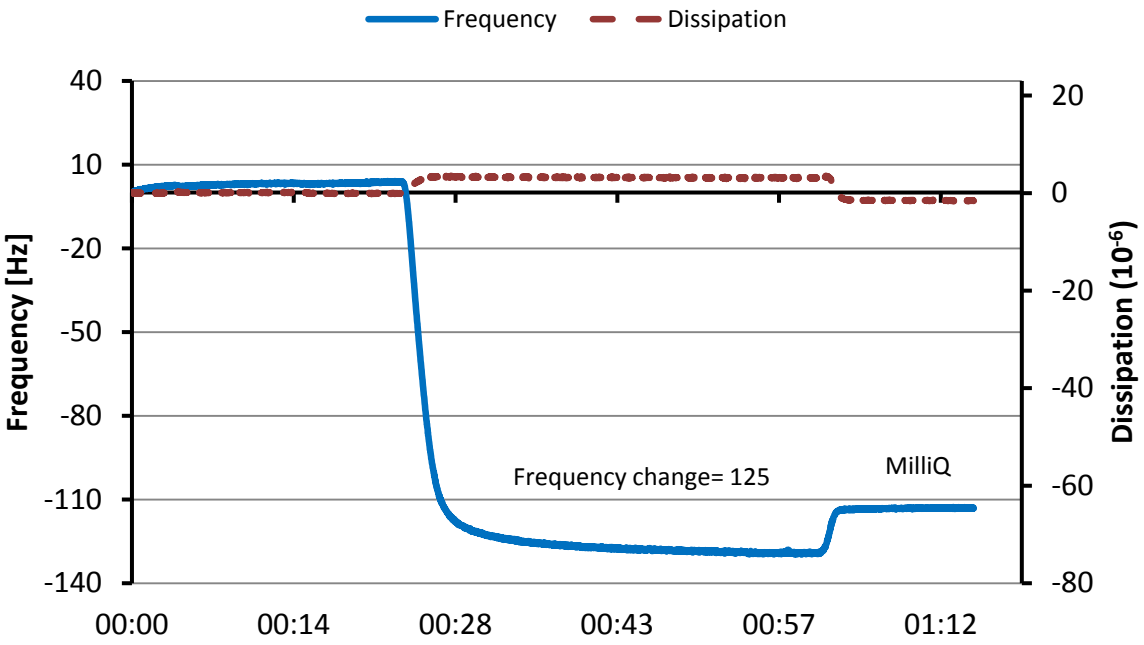

Figure 39 Silica adsorption on NCC/APTMS surface in lower silica concentration (0.004 wt%). Approximate frequency change is 125. The graph is based on the third overtone.

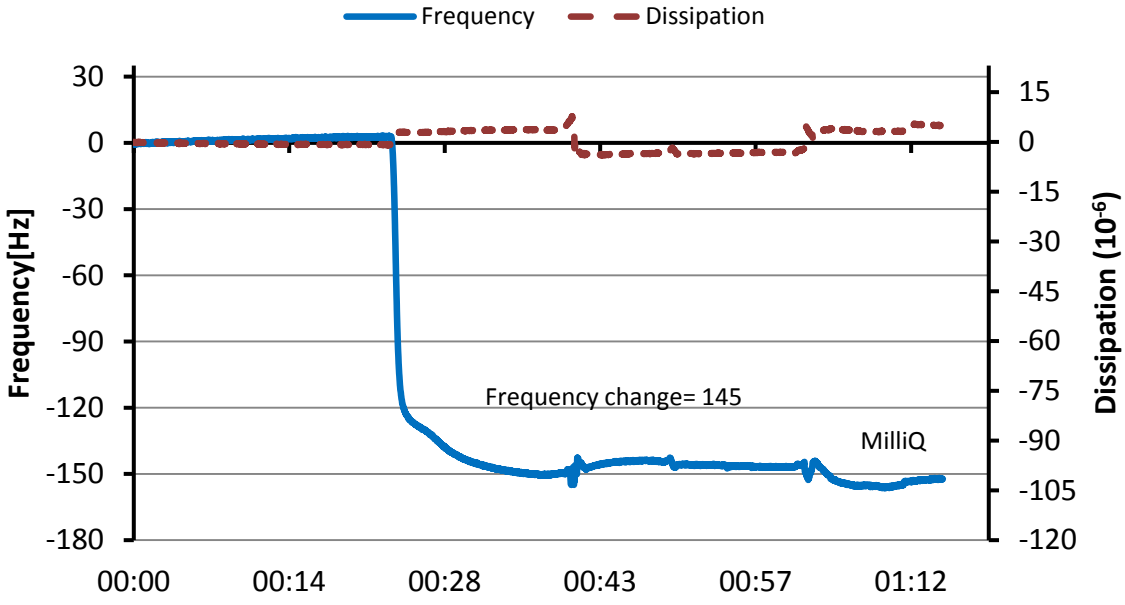

Figure 40 Silica adsorption on NCC/APTMS surface in medium silica concentration (0.04 wt%). Approximate frequency change is 145. This sample showed unstable frequency behavior for a while before the addition of MilliQ. The graph is based on the third overtone.

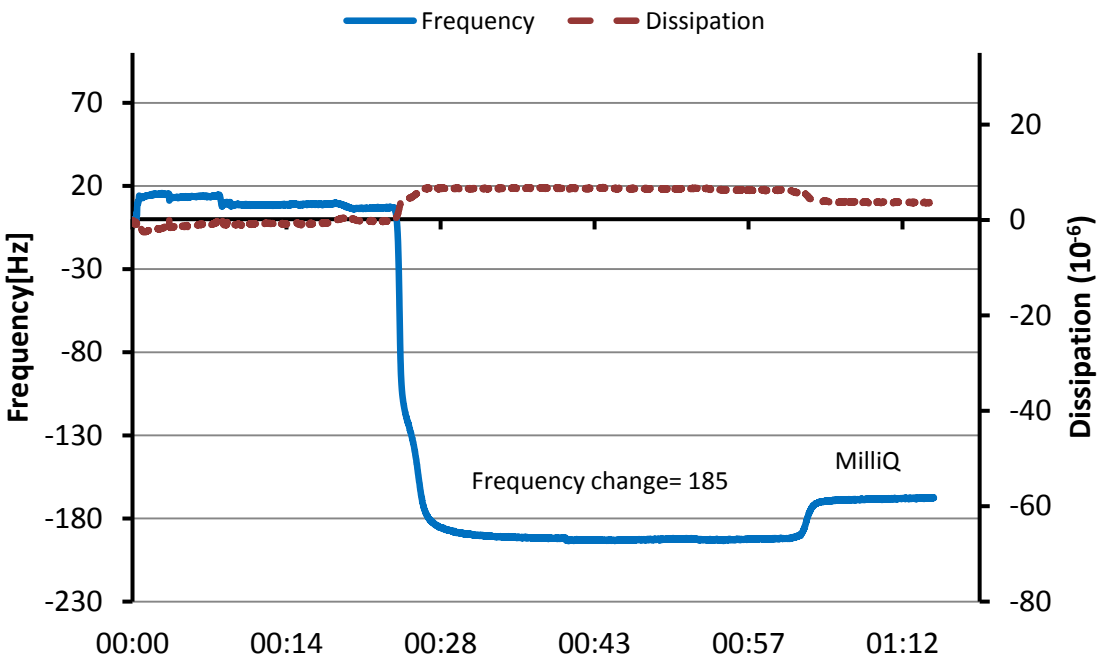

Figure 41 Silica adsorption on NCC/APTMS surface in higher silica concentration (0.4 wt%). Approximate frequency change is 185. The graph is based on the third overtone.

In this test increasing silica concentration from 0.004 wt% to 0.04 wt% firstly increased frequency from approximatly125 to 145 and increasing silica concentration to 0.4 wt% increased frequency to 185.

4.2.3. Section 2-Part 3 Adsorption of silica particles on APTMS surface in different pHs

In this part the trend of silica adsorption on APTMS coated quartz crystals was investigated in three different pHs. Silica concentration was held constant at (0.04 wt %) and the test were started and ended with MilliQ. pHs of silica solutions were respectively pH 7, pH 4 and pH 2 which are illustrated in Figure 42.

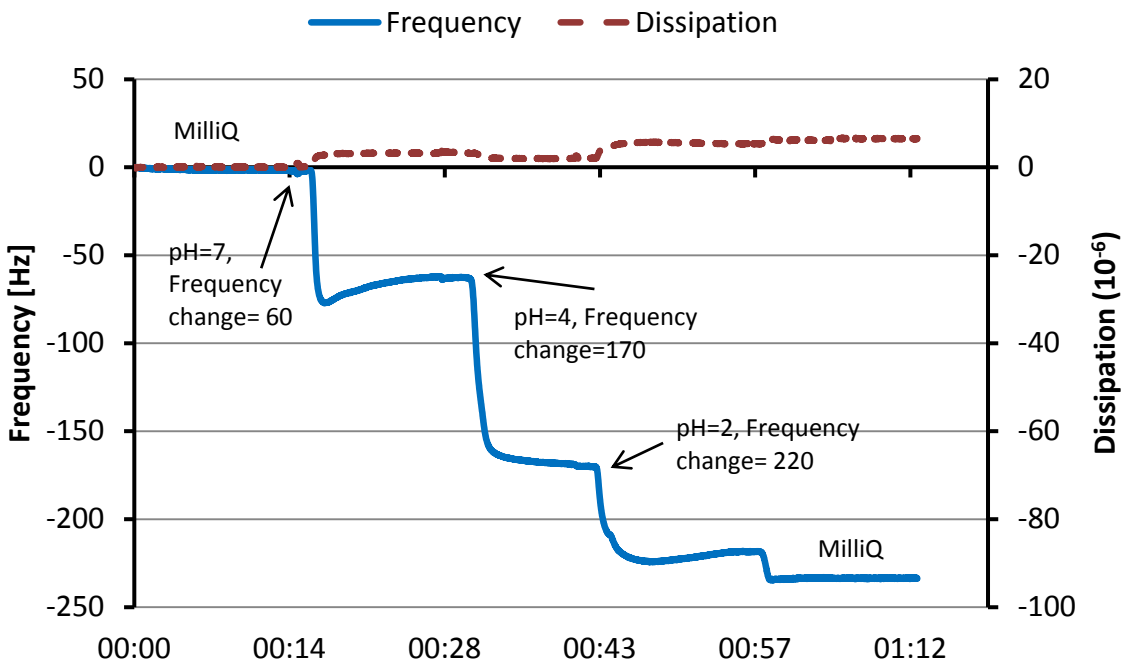

Figure 42 Silica adsorption on APTMS surface in three different pHs with constant silica concentration of 0.04 wt %. Approximate frequency changes are shown for each pHs. The graph is based on the third overtone.

In this test silica particle adsorption on APTMS surface was increasing continually with lowering pH (see Figure 42)

4.2.4. Section 2-Part 4 Adsorption of silica particles on APTMS/NCC surface at varying pH

In part 4 the silica adsorption onto surface coated with APTMS and NCC in three different pHs was monitored. Silica concentration was constant in those three silica solutions (0.04 wt %) and the test was started and ended with MilliQ. pHs of silica solutions were respectively pH 7, pH 4 and pH 2 (The same pHs and the same silica concentration of test part 3) which they are illustrated in Figure 43.

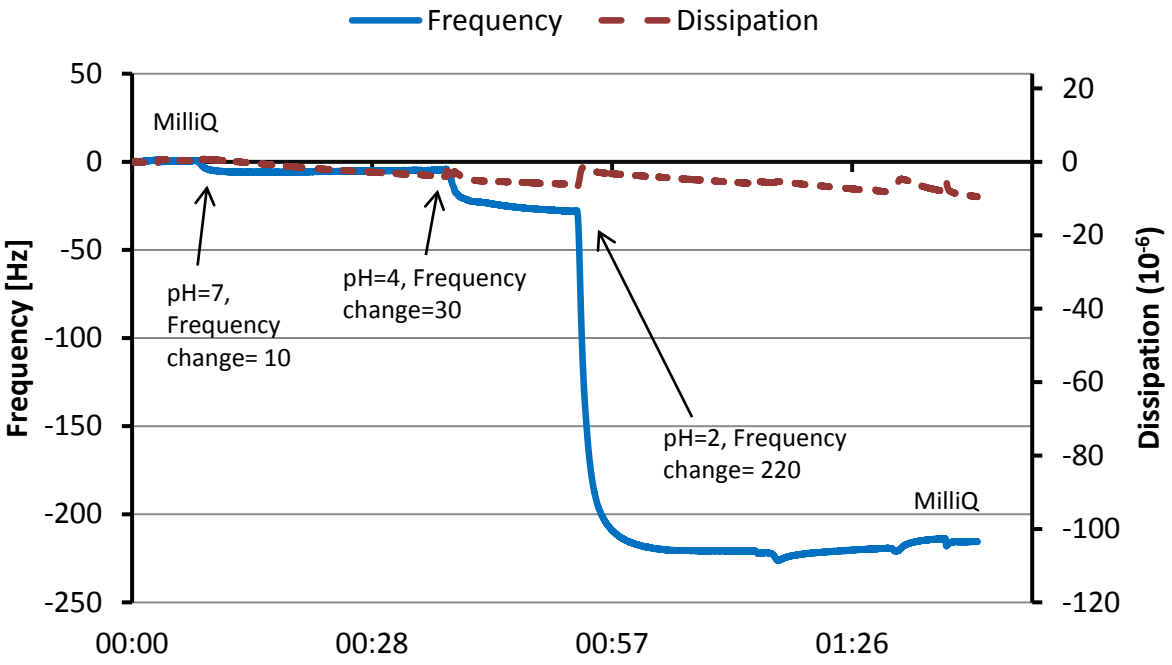

Figure 43 Silica adsorption on APTMS surfaces coated with NCC in three different pHs with constant silica concentration of 0.04 wt %. Approximate frequency changes are shown for each pHs. The graph is based on the third overtone.

4.3. Section 3-SEM image of Nano-cellulose coated surface

The SEM image bellow show NCC fibers spin coated onto a QCM-D crystal surface covered with APTMS (Figure 44). The length of fibers range is between 100-300 nm.

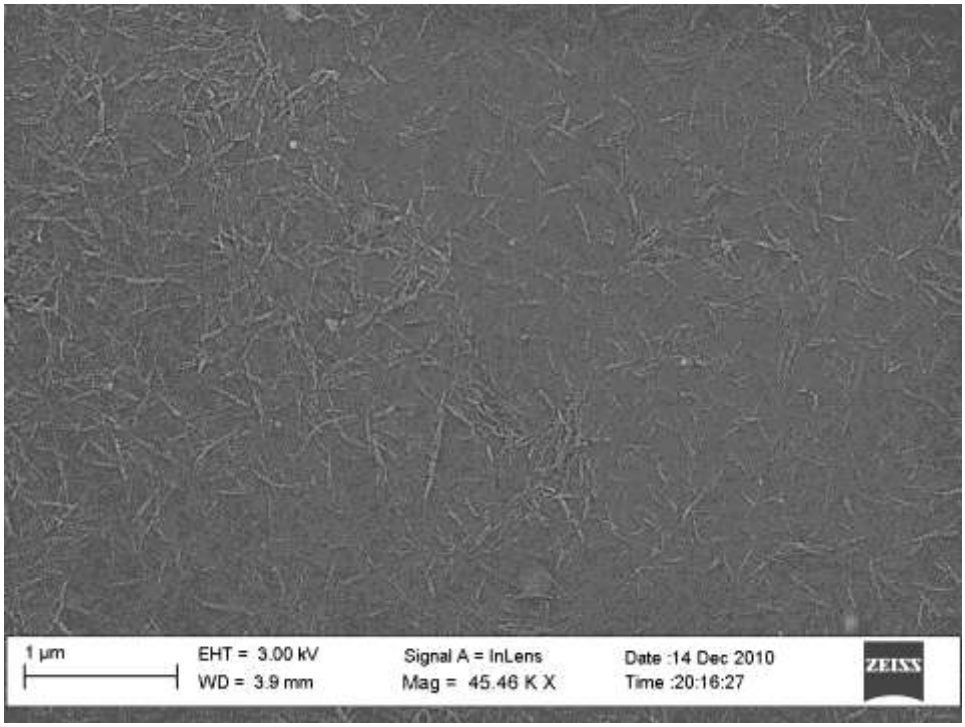

Figure 44 SEM micrographs showing NCC fibers. Length of fibers was roughly 100-300 nm. (Image provided by Christoffer Abrahamsson, Department of Applied Surface Chemistry, Chalmers University of Technology)

4.4. Section 4 TEM micrographs

In this section, TEM images of 7 different gels with 9 wt% silica or silica/NCC at different pH, salt and NCC concentration are shown. The images was taken with the purpose of investigating how for example salt concentration and pH might change micro and nano-structure.

4.4.1. Section 4-part 1 Silica gels

In part 1 TEM images of pure silica gels with two different salt concentrations: 0.5 and 0.9 M in two different pHs: pH 7.8 and pH 4 are shown. For each gel two different magnifications are selected in each row (Figure 45-50). Silica concentration is constant (9 wt %) in all TEM images.

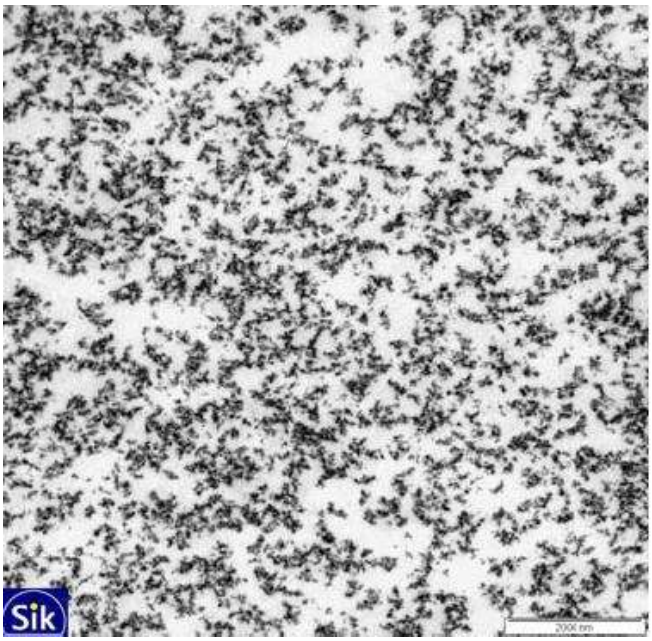

Figure 45 TEM image showing 9 wt% silica gels with 0.5 M NaCl at pH 7.8 in lower magnification

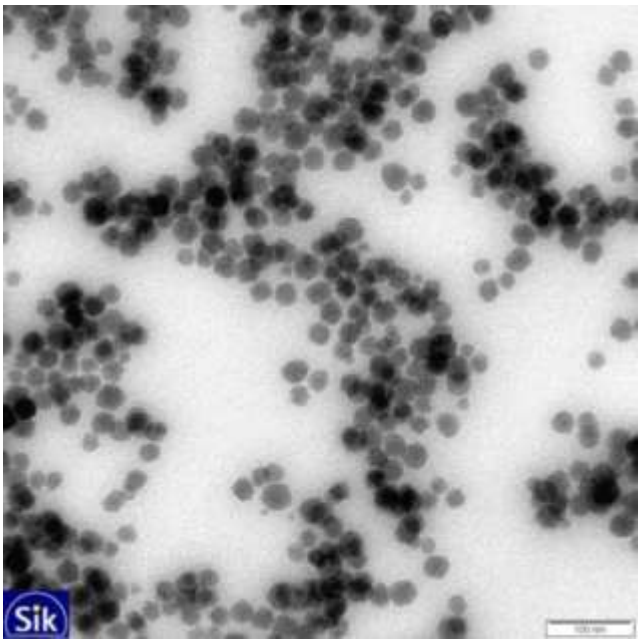

Figure 46 TEM image showing 9 wt% silica gels with 0.5 M NaCl at pH 7.8 in higher magnification

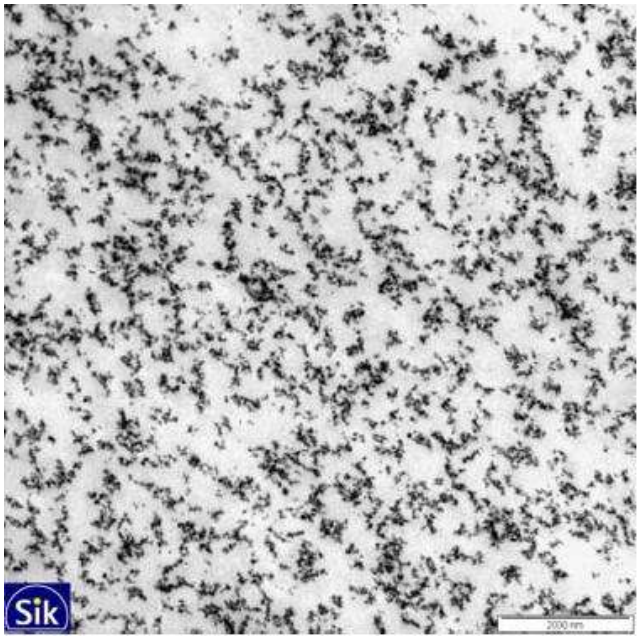

Figure 47 TEM image showing 9 wt% silica gels with 0.9 M NaCl at pH 4 in lower magnification

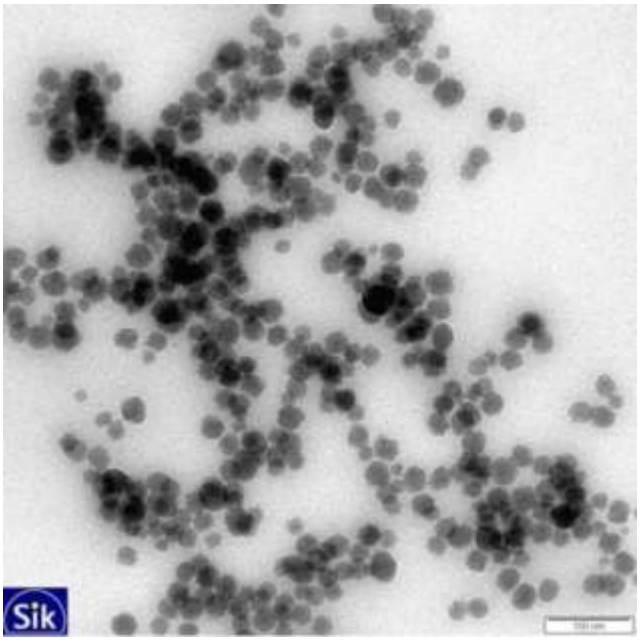

Figure 48 TEM image showing 9 wt% silica gels with 0.9 M NaCl at pH 4 in higher magnification

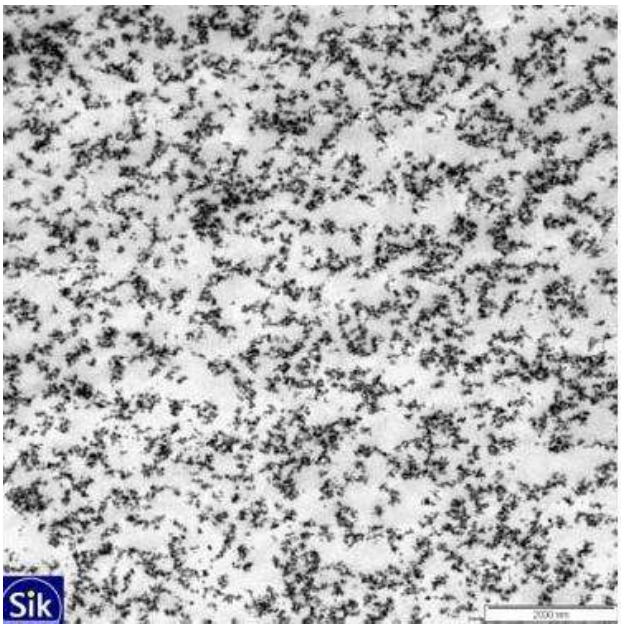

Figure 49 TEM image showing 9 wt% silica gels with 0.5 M NaCl at pH 4 in lower magnification

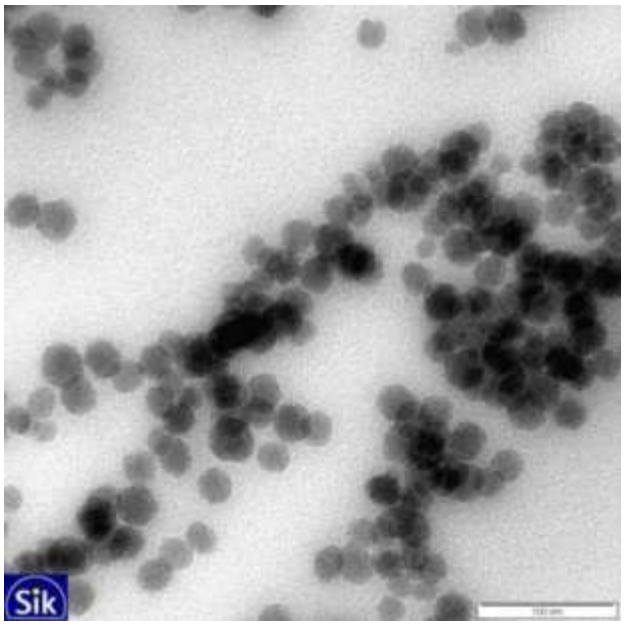

Figure 50 TEM image showing 9 wt% silica gels with 0.5 M NaCl at pH 4 in higher magnification

4.4.1. Section 4-part 1 Silica/NCC gels

In this part TEM images of silica and NCC gels with two different salt concentrations: 0.5 and 0.9 M in two different pHs: pH 7.8 and pH 4 are shown. Similar to previous part, for each sample, one high and one low magnification was selected and illustrated side by side below (Figure 51-56). Silica concentration was constant (9 wt %) for all TEM images.

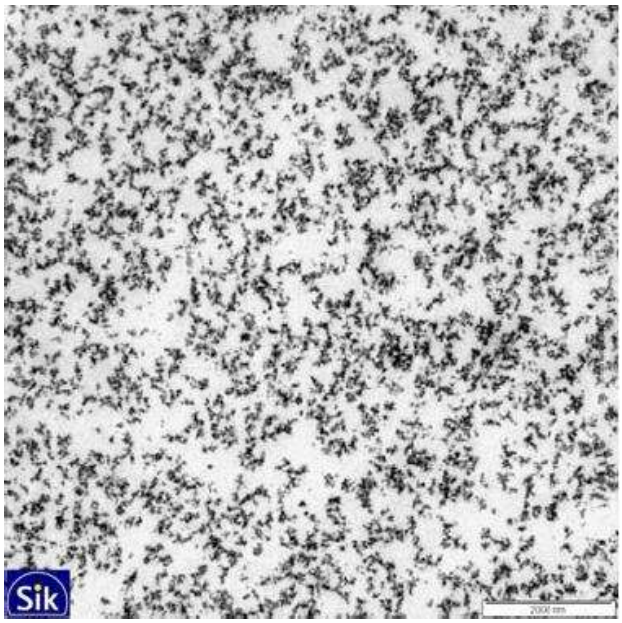

Figure 51 TEM image showing 9 wt% silica gels with 0.1 g/l NCC and 0.5 M NaCl at pH 7.8 in lower magnification.

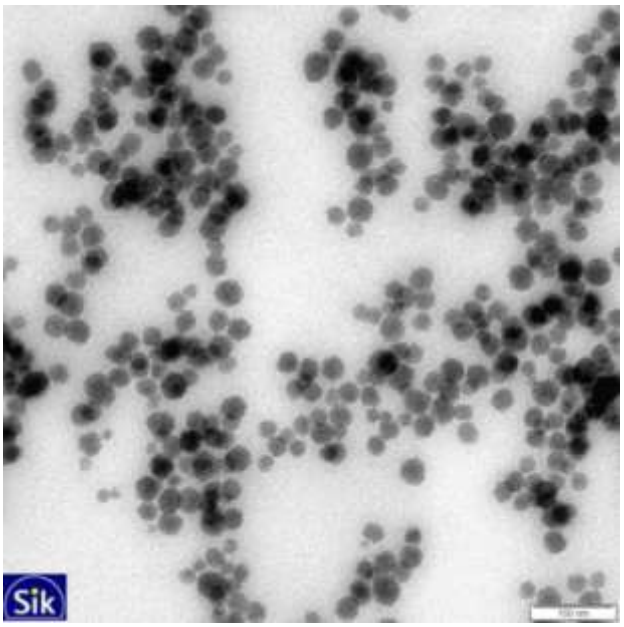

Figure 52 TEM image showing 9 wt% silica gels with 0.1 g/l NCC and 0.5 M NaCl at pH 7.8 in higher magnification.

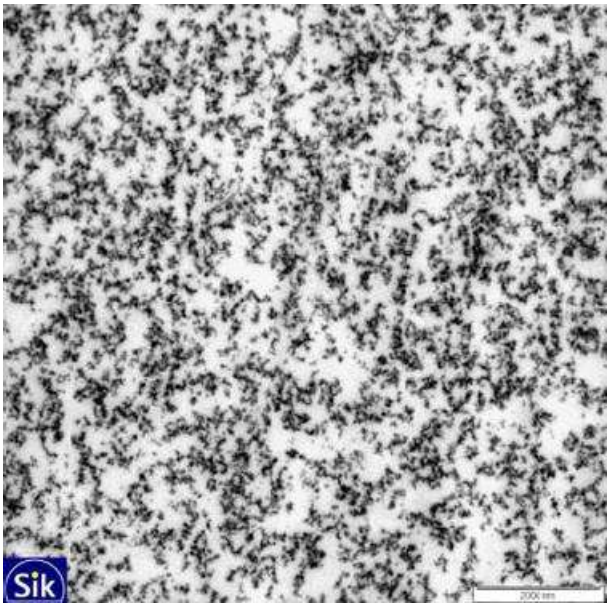

Figure 53 TEM image showing 9 wt% silica gels with 0.5 g/l NCC and 0.5 M NaCl in pH 7.8 in lower magnification.

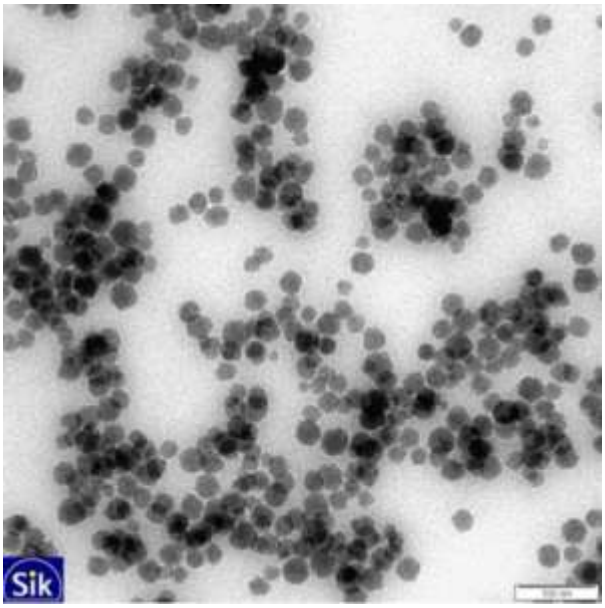

Figure 54 TEM image showing 9 wt% silica gels with 0.5 g/l NCC and 0.5 M NaCl at pH 7.8 in higher magnification.

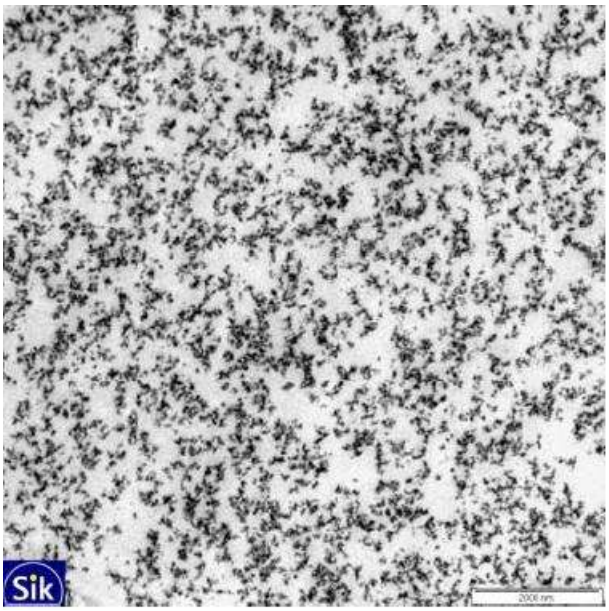

Figure 55 TEM image showing 9 wt% silica gels with 1 g/l NCC with 0.5 M NaCl at pH 7.8 in lower magnification.

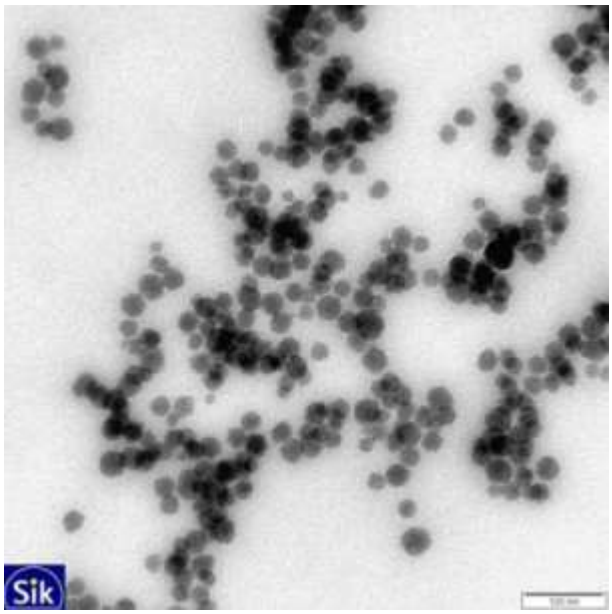

Figure 56 TEM image showing 9 wt% silica gels with 1 g/l NCC with 0.5 M NaCl at pH 7.8 in higher magnification.

As mentioned previously, Figure 45-56 illustrates the micro and nano-structure of seven different silica composite gels in two different pHs with constant silica concentration with a variation of the NaCl concentration. It was expected that pH would results in differences in the structure but such differences was not obvious and notable in the images. For each sample one low and one high magnification is reported here side by side. By visual checking of these images, it seems that at lower pHs and higher NaCl concentration might have slightly bigger pores which may influence diffusion.

4.5. Section 5- Diffusion 1H-NMR results

The self-diffusion coefficient in 16 different gels containing silica in three different pHs and/or NCC particles at one pH was measured with 1H-NMR method. Table 1 presents the self-diffusion coefficients. Diffusion coefficient values did not change so much but by increasing NaCl concentration, diffusion coefficient decreases which will be discussed later. At pH 4, diffusion is slightly higher than pH 6 and pH 7.8. Increasing silica concentration (from 5 wt % to 9 wt %) decreased the diffusion coefficient and addition of NCC also decreased the diffusion values slightly which is logical because of increased obstruction of diffusion.

No	pH	Silica (g/l)	NCC (g/l)	NaCl (M)	Self-diffusion coeff. (1 10^{-9} m^2/s)	D/D_0
1	7.8	9	0	0.9	**1.96**	**0.90**
2	7.8	9	0	0.5	**2.02**	**0.92**
3	7.8	5	0	0.9	**2.00**	**0.93**
4	7.8	5	0	0.5	**2.06**	**0.94**
5	7.8	9	0.1	0.5	**2.02**	**0.92**
6	7.8	9	1.0	0.5	**2.01**	**0.92**
7	7.8	9	0.1	0.9	**1.96**	**0.91**
8	7.8	9	1.0	0.9	**1.95**	**0.90**
9	6	9	0	0.9	**1.83**	**0.85**
10	6	9	0	0.5	**2.09**	**0.95**
11	6	5	0	0.9	**2.08**	**0.96**
12	6	5	0	0.5	**2.15**	**0.98**
13	4	9	0	0.9	**2.02**	**0.94**
14	4	9	0	0.5	**2.17**	**0.99**
15	4	6	0	0.7	**2.10**	**0.97**
16	4	5	0	0.9	**2.12**	**0.98**
	H2O	___	___	___	___	
	H2O + low salt	___	___	0.5	**2.19**	

	H2O + high salt	___	___	0.9	**2.16**	

Table 1 Self-diffusion coefficient for16 different gels

Higher silica/NCC concentration reduced the diffusion coefficient (see Figure 57)

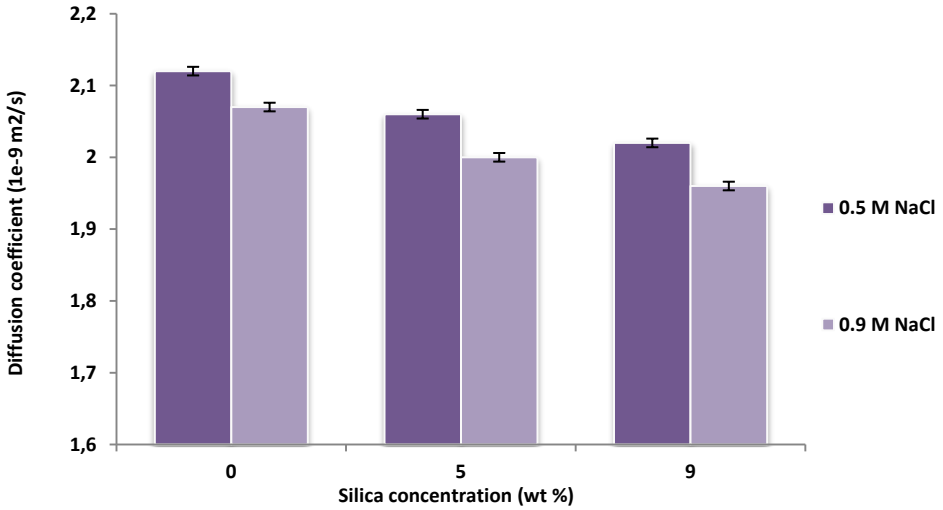

Figure 57 Self-diffusion in silica gels in different silica concentration at pH 7.8

Decreasing pH increased the diffusion coefficient in the silica gel system. The effect of pH on diffusion in gels with 5wt% relative 9wt% silica is illustrated in Figure 58. By changing pH from 7.8 to 4, diffusion coefficients increased by around 7% (Figure 58).

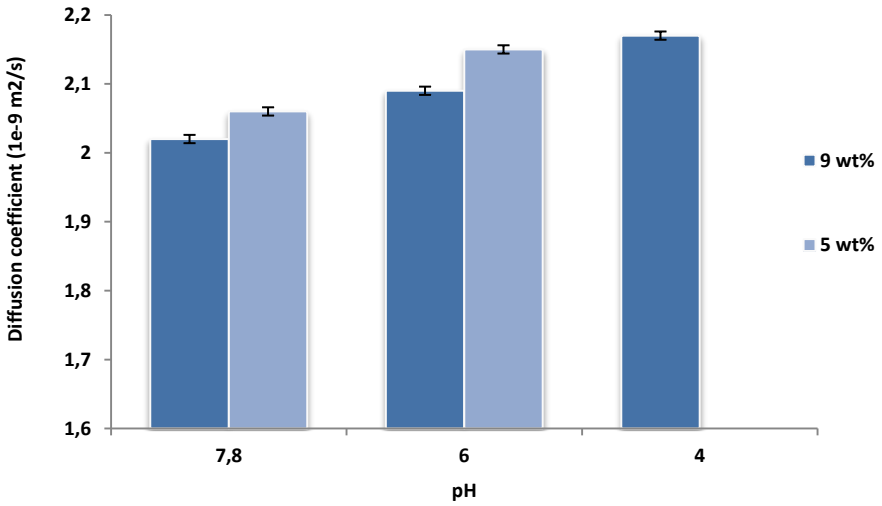

Figure 58 Self-diffusion in silica gels with three different pHs in two different silica concentrations (5 and 9 wt %) and constant salt concentration, 0.5 M NaCl. (The missing point is a solution with 5wt% silica and 0.5 M NaCl at pH 4 which never gelled)

Chapter 5 Discussion

This work has been focused on understanding the mass transport in nano and micro porous materials. Gelation conditions were varied in order to study how this would affect the formation of different micro/nano structures [20]. In order to do this a library of different silica gels were created and the phase behavior of pure silica gels and silica/NCC gels were monitored at different time points. After this the next step was to obtain TEM images from the particle gels. Mass transport consists of two phenomena; diffusion and flow. Diffusion was measured with 1H-NMR but flow measurements were not within the scope of this study. To facilitate understanding of the interparticle forces between silica and NCC particles in the sol and the gel, QCM-D was used. In the following discussion the results are interpreted side by side with the previous literature studies trying to elucidate the nano/micro structure and mass transport properties relationship.

5.1. Pseudo-phase diagrams and the logic behind selection of variables

In general during the process of going from sol to gel (destabilization) different phenomena occur at the same time. Specifically the sol-gel transition of silica may be rather complex because at one hand there is a competition between attractive (e.g., van der Waals) and repulsive (e.g., electrostatic) forces between the particles. On the other hand there is the formation of covalent siloxanes bonds (condensation reactions) where high pH favors covalent bond formation while very high breaks them. In addition, there are more factors that affect gelation, such as diffusion of particles that depend on size and density of the particles and entropy forces [10, 16, 18-20, 27-34]. Changing the interparticle potential from highly repulsive to less repulsive causes destabilization of the colloidal system. This study used two different methods to induce gelation: shifting the pH (ΔpH method) that reduces the surface charge and screening the surface charges by increasing ionic strength (ΔI method) both methods makes it more likely for the particles to aggregate [16, 20, 31, 32]. Therefore, pH and salt concentration were selected as two logical variables in the phase diagrams of this study.

Based on Iler's well known diagram (Figure 4) three different pHs with three different gel times were selected in this study. In Figure 4 it can be seen that pH 6.0 gives the minimum gel time while pH 7.8 and pH 4.0 both have longer relative gel time. Accordingly, the minimum gelation time for silica tend to be around pH 6 [18, 32]; Besides, It should be noted that L. Lench et al. also showed different pHs would lead to various micro/nano structure in the gels and they found that acidic conditions resulted in more linear structures in the created silica gels contrasting with basic conditions that resulted in more branched structures [16, 33].

For increasing ionic strength, NaCl salt was selected but other salts has been used in literature and they have showed to give differences in the gelation caused by their different sizes and charges. [31, 34-36]. The range of NaCl concentration that was investigated was 0.01-0.9 M and was deemed suitable to avoid precipitation of slat in the gel structure but still have fast enough gelation. Moreover, different particle content in a created particle gels will change the porosity and micro/nano structure of the created gel [20] The range of silica and NCC concentration was selected from 1-10 wt% and 0-3 g/l respectively because these volume fractions were similar to many of the materials used by the SuMo companies.

5.1.1. Gelation in pure silica system

Zackrisson et al. [20] reported that higher ionic strengths (with NH_4HCO_3 salt) are required to reach gelation in less concentrated silica sols and vice versa. The pH used in their experiments was around 9.2 and the particle size was around 8 nm. In this thesis work slightly or much lower pHs was used together with larger silica particles (20 nm). Despite these differences, pseudo-phase diagrams in this study display a similar trend as Zackrisson's stability diagrams with respect to silica and salt concentration [20, 28].

In day 60 at pH 7.8 (Figure 9-12) and also at pH 6.0 (Figure 13-18) minimum silica concentration for gelation was 3.0 wt % but at pH 4.0 this value increased to 6.0 wt % (Figure 19-22) and it means that at pH 4, the silica sol is more stable than at higher pHs. This result is consistent with result of Kobayashi et al. that used particles of similar size (around 30 nm) and KCl salt with similar ionic strength (0.5 M). They also found that at pH 4, aggregation rate is notably lower than aggregation at pH 6 or pH 7.8 [19].

In this study, the minimum required NaCl concentration for gelation is 0.3M at pH 7.8 and pH 6.0 but this value is 0.1 M at pH 4.0. J. Depasse et al. also reported that increasing pH, would increase required cation concentration for aggregation and gelation [32] because at higher pH, there are more charges on the silica surfaces so there are stronger repulsion forces between the silica particles; therefore, in order to screen the electrostatic interactions, more NaCl concentration would be required. Not only NaCl but also other salts have the same effect on the silica surface, e.g., in Zackrisson's study, NH_4HCO_3 have approximately the same value for the minimum required salt concentration for aggregation as in this thesis work. This similarity might be because that ammonium and hydrogen carbonate has (+1) and (-1) charges respectively, same as sodium and chloride ions in NaCl salt. For 5-10 wt% silica the required concentration for gelation is NaCl was around 0.3 M [20] which is in the range of current study (0.1-0.3 M NaCl).

In this study, relatively monodisperse silica particles were studied at rather low silica concentration (1-10 wt %). The aggregation of silica with different particle size distribution in a higher range of silica concentration (12-36 wt %) has been recently studied by A. Johnsson et al. [8]. Their most important finding was that the initial shape of the particles, free particles or preaggregated had big effects on growth of the aggregates. Due to higher range of silica concentration, and different criteria for gelation observation they reported gelation time between 43-47 min. In Johnsson's study the gelation time was determined visually as the time at which the gel surface was stationary when the tube containing the reaction mixture was turned upside down. In this study strong gels were needed for successful embedding and microtoming for TEM imaging. It is unclear how strong the gels were in A. Johnsson et al.´s study compared to the ones in this study. It should be also noted that pH range in their study is 9.6 to 10.1 with the constant salt concentration around 0.3 M NaCl which is approximate the same with this study [8].

Gel formation at pH 4 exhibits a significant delay for the gel formation compared to gel formation at pH 6 or pH 7.8. This result was similar to the results illustrated in Iler's figure (Figure 4) but there is a deviation. Iler noted that the relative gelation time is controlled by the rate of collisions processes and the formation of covalent bonds[16]; Accordingly, going from pH 3-6 the gel formation rate increases; in contrast, going from pH 6-8 this rate decreases [16]. Presence of H_3O^+ in the solution

increases the hydrolysis reaction rate and presence of OH^- ions increases the rate of condensation reaction[33]. The relative gel times for the three different pHs in this study showed a slight shifting in pH for the gel time minima (Figure 59) compared to Iler (Figure 4). The reason for this can be an increased likelihood of covalent bonding formation at higher pHs relative Iler´s results. It could also be that the likelihood of collision was higher at high pH compared to Iler. If one speculates about the reasons for the shift in the balance between the above mentioned forces it can be because of anything from impurities in the silica sol, different particle roughness, particle size and particle size distribution [17-20, 33, 37, 38].

It should be also noted that there is no absolute pH position of the relative gel time curve in Iler's figure. The figure just gives an approximation and comparison between different gel times in different pHs and salt concentrations.

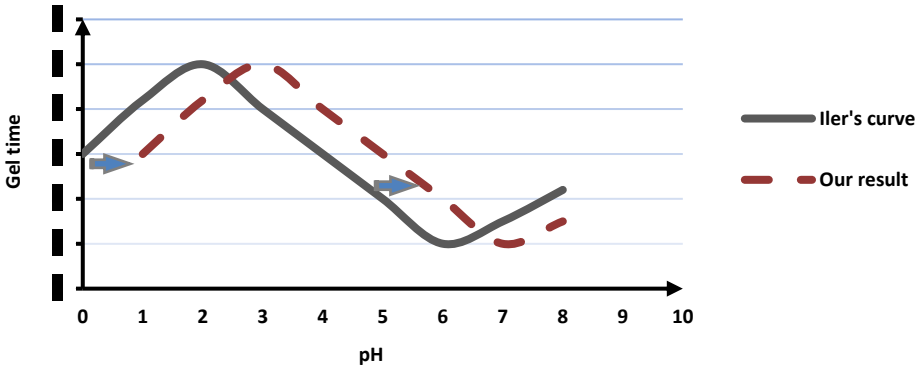

Figure 59 shifting in gel time from Iler's figure

According to this shifted curve (dashed line in Figure 59) minimum gel time is not at pH 6 and gel time is longer at pH 4; moreover, gel time at pH 6 is slightly longer compared to pH 7.8 (see figures 12, 18 and 22).

5.1.2. Gelation in NCC system

When looking at gelation in the pure NCC system (Figure 23-24) only one observation was made after one day at which there were no gelled samples. However, there were semi-gels that were not mechanically stable. Thus the pseudo-phase diagram (Figure 24) for pure NCC has a zone of semi-gel instead of gel. There are many studies about gelation of NCC in literature which is discussed very shortly here side by side with the findings from this study.

First, the reason that there is not a strong gel in the pure NCC system was that there was no covalent bonds between the NCC fibers instead there is hydrogen bonds and van der Waals forces was not strong enough to results in a gel according to the definition in this study [39]. The definition of a gel

was pretty strict in this study as a sample has to be able to remain intact after the inverted tube test which was a test that applies a reasonable high force on the gels. In many other studies made what this study calls semi-gels might be considered gels because of a less demanding rheological definition of the term "gel".

Secondly, a new phase behavior marked by a viscous flow behavior compared to a sol and referred to as "viscous" was found in NCC system, this rheological behavior was not present in the pure silica system. The viscous region was seen between 1-1.5 g/l NCC and above this concentration there is semi-gel region. According to literature the minimum NCC concentration for a viscous behavior was [40] ca. 3 wt% but in sometimes it is as low as 0.5 wt% NCC [39]. Viscous behavior in NCC system will be discussed more later.

NCC concentration changes the behavior of the system. Below 0.5 g/l NCC, all samples are fluid and viscosity has not yet been increased (Figure 23) but in the range of 1-1.5 g/l NCC most of the samples flow hardly and viscosity increases significantly and finally between 2.5-3 g/l NCC most of the samples was semi-gels (Figure 23-24). The range of cellulose concentration for changing the phase behavior depends to a large degree on the charge density and different preparation method may introduce different functional groups with different charge density moreover, the size of rods will influence on the rheology of suspension. Typically large rheological differences would be found at 1-10 wt% NCC in aqueous medium [39]. In literature minimum concentration for gelation is different depending on the source of cellulose, preparation conditions and aggregation conditions (ionic strength and type of ions, etc.) but in general gelation in NCC solutions is reported in the range of 1.0-3.0 wt% NCC [39-43].This is higher than the highest NCC concentration that was used in this study (0.3 wt% for 0.3 g/l).

There are also many studies about the effect of salt concentration on the phase transitions of NCC suspensions out of which two was done by J. Araki et al. [40] and X. dong et al. [44]. According to their findings traces of salt (0-2.5 mM NaCl) cause a remarkable change in phase behavior of NCC suspensions. Accordingly the minimum salt concentration explored for changing the phase behavior in a NCC suspension is about 10 mM which in this study this concentration reach to 0.7 M which is much higher comparing to mentioned studies. Dong's study shows that composition of the isotropic and anisotropic phases would be changed as a function of electrolyte concentration where both coexist and increasing the amount of added salt decreases anisotropic phase formation and chiral nematic pitch was found to decrease and phases became more highly twisted in this system and this is because of the decrease in the electrical double layer thickness [39, 44].

5.1.3. Gelation in silica/NCC system

The investigation of gelation in the mixed silica/NCC system was performed in two different conditions. Firstly, silica concentration and pH was kept constant at 5 wt% and pH 7.8, and NCC and NaCl concentration was varied (illustrated in Figure 23). In the second case, NaCl concentration and pH was kept constant at 0.5 M and pH 7.8 respectively and silica and NCC concentration was varied. This was done at both pH 7.8 and 9.25, i.e., the original pH of stock colloidal silica.

In the case of constant silica concentration (see Figure 25-27), after one day all samples at 0.6 M salt and above became gels (Figure 25) and after 30 days all sample at 0.25 M NaCl and above were gels (Figure 27). The role of NCC in the gelation process in this system was not the same as silica and it seems that silica plays the main role in the network formation and it seems to be because of strong covalent bonding between silica particles. The number of samples with the viscous behavior also decreased over the time and it seems that viscous behavior in this system is transient (compare viscous points in the different time points in Figure 25-27).

In the second case, (with constant salt concentration), silica and NCC varied from 0-1 g/l and 0-9 wt %, respectively. At pH 7.8, samples with 9 wt% silica displayed gel in day one (Figure 28) and gel region expanded to 7 wt% silica in day 27 (see Figure 29-30). NCC concentration did not result in a significant change in the gel region (see Figure 28-30). The viscous state only existed during day one. However, the semi-gel state persisted to the end point. At pH 9.2 the gel time is notably shorter and after one day many gels were formed and after 13 days system reached to its steady state situation (except for biphasic samples). Viscous behavior again is a transient behavior in the pseudo-phase diagrams (Figure 31-35), i.e., all samples with 3 wt% silica displayed a viscous behavior at the beginning (Figure 32) and they transformed to the other phases later (see Figure 32-35).

5.1.4. Gelation in different systems

Viscous flow behavior

The first difference between the phase behavior of a pure silica system and mixed system was the presence of viscous behavior in the presence of NCC. This is a consequence of the interparticle forces between NCC fibers. The origin of these forces could be hydrogen bonds between NCC rods. In addition, NCC rods orientation in presence of counter ions may cause this effect which is called electroviscous effect in literatures [39, 45]. In another study which was conducted by H. Ono et al, viscosity of NCC suspension was studied by the help of 1H-NMR method [45]. H. Ono concluded that extraordinary high viscosity of NCC suspensions is due to network generation. In his study similar to this study the size of rod-like NCC was 100-300 [45].

Moreover, based on observation, viscous behavior was a transient (temporary) behavior in the mixed system of silica/NCC (see Figure 25-35). Viscose sols subsequently transformed to the stable phases (gel or biphasic). The transient behavior was most likely because of more network formation between silica particles. The process possibly could be a result of/or be affected by van der Waals

and hydrogen bonds between NCC-NCC [39] moreover it can be because of ‘bound water’ according to H. Ono et al. study[45].

Crowding and synergic effects

A comparison between minimum required salt concentration in the pure silica system and silica/NCC system with the same silica concentration and pH, i.e., 5 wt% silica and pH 7.8 respectively, shows that in presence of NCC changes minimum salt concentration for gelation from 0.5 M to 0.25 M. Gelation in the mixed system is complex; but it is likely that the crowding effect was the main reason for gelation at a lower salt concentration. As described by A. Celzard et al. the crowding effect of fiber particles in the system of suspended fibers is assumed to cause a transition from non-connected to connected particles [46]. Therefore, this crowding effect can be one reason for the mentioned difference between silica and silica/NCC system. Moreover, addition of NCC fibers to a colloidal silica system increase overall concentration of particles in that system; consequently, connectivity would be increased in the concentrated system between silica particles or aggregates and NCC fibers and it can be a result gelation with the lower salt concentration (compare Figure 9-11 with Figure 25-27).

In the pseudo-phase diagrams of the silica/NCC system, it was observed that a steady state phase behavior was attained faster compared to the pure silica system. Crowding effect may be the reason again for this; however synergic effects due to presenting of two-component mixture (silica and NCC) can be the second reason. Synergic gelation effect (SGE) is reported by Z. Dzolic et al. for a two-component gel (bis-amino acid and bis-amino alcohol) and gelation efficiency and phase transition diagrams of the mixed system were compared with the single component systems[47]. Although those components were difference with silica and NCC but there are some similarities which the main one is existence of hydrogen and also covalence bonds between single particles. Dzolic quantitatively and qualitatively reported that different particles may present the supramolecular (non-covalent) variant of molecular (covalent) copolymerization during gelation and it gives gels of dramatically different properties than those formed by each single component because of different sol-gel transitions[47]. Those dramatic differences exhibited in the current system in terms of gelation times and required salt concentrations. An additional point that needs to be noted is that the mechanism of gelation in Dzolic’s system is similar with particle gelation which is done in this study. In other words, gels form by the self-assembly of the gelator molecules into fibrous aggregates until these aggregates become sufficiently large (now these aggregates can be called “particles”) then, these aggregates interconnect with each other and form a three dimensional network capable of immobilizing the solvent like other type of gels, i.e., silica/NCC gels[47-51].

5.1.5. Phase separation

Viewing the phase behavior of the studied systems (Silica and/or NCC) showed us that probably there are two steps in the gelation process. These two steps are aggregation and then followed by interconnection. This model was described by Morbidelli et al.[29, 30] and supported recently by A. johnsson et al. also in their study of the gelation of silica in presence of NaCl salt [8]. The model of the theory is schematically shown in Figure 60 The gelation process according to this model starts by the aggregation process (middle drawing in Figure 60) and the aggregates diffuse freely until aggregation process is arrested because of spatial restrictions or lacking single particles in the solution. The particle network spans the entire system volume and the mechanically stable gel is formed (right drawing in schematic Figure 60). Semi-gel points, viscous points and two-phase separated points in all pseudo-phase diagrams (Figure 9 to Figure 35) seems to be involved in this step (aggregation step). In the phase separated samples the system is not substantially crowded by the aggregates and they will therefore fall to the bottom of tubes because of the gravity forces (Figure 11 to Figure 35).

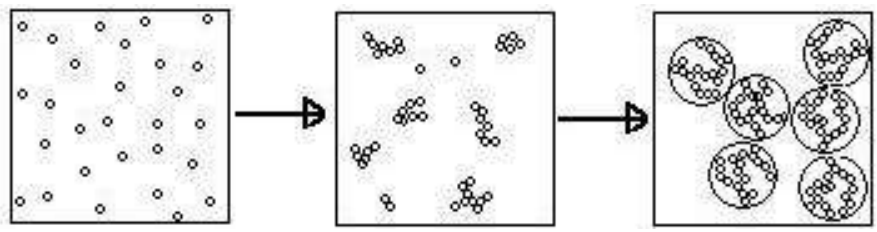

Figure 60 schematic of aggregation process in silica colloid followed by interconnection of clusters (secondary particles) and caged aggregated which represent gel points in this study (redrawn from ref. [52])

5.1.6. Phase separation in silica system

Phase separation in pure silica system was seen at different pHs and different salt/silica concentrations and can be seen in Figure 11, Figure 16-17 and Figure 20-21 for pH 7.8, pH 6.0 and pH 4.0 respectively. In order to have phase separation a minimum salt concentration is needed (similar to gelation) however silica concentration should not be above a certain value. This values depends on pH. This finding is consistent with the two-step mechanism of gelation (Figure 60) that was explained above. At pH 7.8 and pH 6.0 maximum silica concentrations and minimum salt concentrations are 2 wt% silica and 0.3 M NaCl. But, at pH 4.0 the biphasic region did not appear until higher silica concentration (5 wt% silica) and lower salt concentration (0.1 M NaCl); The biphasic region was significantly bigger in the lower pH.

As described before, in the gelation process of colloidal silica there is a competition between collisions of particles (i.e., collision is more effective in the lower pH due to charge screening) and the covalent bonding of the silica particles that is limited in the lower pH [10, 16]. Consequently at

pH 4, silica particles can collide with each other effectively but bonding between particles is less likely. It is therefore possible that when the larger aggregates has formed these have hard to interconnect at low pH, maybe because of their higher mass and the aggregates will therefore drop to the bottom.

In biphasic samples, the relative amount of the lower phase was related to silica and salt concentration, e.g., At pH 7.8 (see Figure 11) at 1 wt% silica and 0.3 M NaCl, 20% of the sample volume was occupied by the lower phase but at 3 wt% silica with the same salt concentration 75% was occupied by the lower phase and this percentage increased to 90% at 3 wt% silica and 0.7 M NaCl. Both pH 6 (Figure 17) and pH 4 (Figure 21) have the same trend as seen at pH 7.8. At the same silica and salt concentrations lower phase percentages, respectively are 30%, 60% and 80% at pH 6 and 15%, 30% and 35% at pH 4.

Phase separation in the pure silica system did not only develop from the sol phase but also from the semi-gel phase (e.g., see Figure 10-11) and it could even be seen in the gel phase in some samples. In the semi-gels and the entangled aggregates with weakly bonds between each other might be the cause of the semi-gel behavior (mechanically unstable gel), however in the semi-gels that phase separated Brownian and gravity forces can overcome to these weak bonds over time. In this case, afterwards, these aggregates separate from the solution gradually. It should be noted that the lower phase in these cases had a similarity to a gel and this phase did not behave as the lower phase in samples where the aggregates sedimented from a sol where the lower phase behaved more like sand sedimented in water.

5.1.7. Phase separation in NCC system

In this project no phase separation was observed in the pure NCC system, after one day (Figure 23) although in literature phase separation and self-assembly of NCC has been shown; i.e., Y. Habibi et.al reviewed self-assembly and phase behavior of NCC in aqueous and organic mediums under different conditions. According to Habibi et al.'s review, phase separation of NCC in an aqueous medium is a slow process that needs more than one day time at the similar conditions to occur (between 2-7 days) [39, 40]. Moreover, mechanism of phase separation in NCC system is different to the silica system. In a NCC cylindrical dimension, orientation and asymmetry of NCC fibers play their roles in the phase separation; i.e., reducing surface charge of NCC rod can change the efficient rod shape from a straight rod to a twisted rod [39]. Therefore, twisting factor influence on the self-assembly and phase separation process. J. Araki reported that NCC suspension in the presence of very low concentration of NaCl is separated into the upper isotropic and the lower anisotropic phases due to these mentioned specifications [40].

5.1.8. Phase separation in silica/NCC system

In the mixed system, phase separation occurred at pH 7.8 and 9.25. In the first silica/NCC system with the constant 5 wt% silica (Figure 25-27), there were no biphasic samples as expected, because in the pure silica system with the same pH there was only biphasic samples at low salt concentration (see Figure 11) But since no phase separation was observed even at low NaCl concentration in the presence of NCC it is possible that in the presence of NCC fibers gives a crowding effect that hinders the separation process.

In addition, comparison of biphasic samples at pH 7.8 (Figure 28-30) and pH 9.25 (Figure 31-35) shows that silica concentration was more influential than NCC (at least in the current high silica concentration and relatively low NCC concentration). In other words, there was a line between biphasic samples and semi-gel/gel samples vertically in all pseudo-phase diagrams (see Figure 25-35) in a certain silica concentration depending on pH and time-point; e.g., at pH 7.8 this borderline was at 3 wt% silica and at pH 9.25 this line is at 1 wt% silica; in contrast there is no a distinct line horizontally which separate phase behaviors depending on NCC concentration. However, it should be noted that at pH 7.8 after the inverting tube test in day one (Figure 25) biphasic samples with 3% silica converted to semi-gel state in the observation in day three (Figure 26) and stay in that state until day 27 (last observation) which seems hindrance of phase separation after day one is due to interconnection of aggregates after the mixing.

In the silica/NCC system similar to the pure silica system, the relative volume of the lower phase also depends on particle concentration and by increasing of silica and/or NCC concentration the lower phase will grow.

5.1.10. Shrinkage in silica system

Shrinkage was another common behavior in the pseudo-phase diagrams in this study. In brief, shrinkage is a result of new connections and bond formation after the gel point and it causes contraction of the gel network and resulting expulsion of liquid from the gel pores:

$$\equiv Si\text{-}OH + HO\text{-}Si\equiv \rightarrow \equiv Si\text{-}O\text{-}Si\equiv + H_2O$$

Oswald ripening process is another important reason for the shrinkage especially in the silica system [22, 33].

G. Scherer studied shrinkage behavior for titania and silica gels theoretically and experimentally [22, 53]. According to his study the condensation reactions in silica is very sensitive to pH; therefore, it is expected that the rate of shrinkage depends on the pH in a large extent. For example Scherer showed

that shrinkage is minimum at the low pHs because condensation reaction is lower at the low pHs near to the isoelectric point (e.g., pH≈2 for silica) [22]; but, in our experiment, there was a tendency for shrinkage even at pH 4 where at least four samples shrank. This finding in this study could be because of Oswald ripening which is likely to occur more or less depending on pH and due to higher solubility of silica in the higher pHs, Oswald ripening is also increased in the higher pHs.

In this study for pure silica system at pH 7.8, the gel region was growing from 3-20 days and withdraws in day 60 (Figure 12). At pH 6 the gel region is growing from 3-13 and withdraws in day 60 (Figure 18) and at pH 4 from day 3 to day 13 and again from day 13 to day 60 there are two withdraws (Figure 22). Furthermore, it was observed that shrinkage in this system occurred near the gel region borderline. In other words, shrinkage did not occur in gels with high silica/salt concentrations apparently due to higher mechanical stability of gel network in those gels.

5.1.11. Shrinkage in NCC system

In this study, samples with pure NCC system were observed for one day and no shrinkage was observed. In literature there are many studies about swelling of NCC hydrogel [54, 55] and according to other studies NCC gels have very low shrinkage behavior [56] Since cellulose has next to no solubility in water systems no Oswald ripening can be expected that could cause shrinkage, hence shrinkage in wet conditions is unlikely in the pure NCC system.

5.1.12. Shrinkage in silica/NCC system

No shrinkage was observed in the mixed silica/NCC system up to 30 days. However in silica systems no shrinkage was observed at this time point nether. Hence it is not possible to say if the NCC would affect shrinkage. However, it is possible that the NCC fibers could provide structural hindrance for shrinkage at later time points.

5.2. Silica and NCC interactions with QCM-D method

The interaction between colloidal silica and NCC fibers was studied at different pHs and silica concentrations of the QCM-D method.

In the experiments NCC covered QCM-D crystals was exposed to colloidal silica dispersions. As a control, surfaces covered with positively charged APTMS were used. This was the same surface that the NCC fibers were anchored to. When exposing the surfaces to colloid silica dispersions at different pHs, adsorption differed. By exposing APTMS surface to decreasing pHs adsorption of silica particles increases gradually and this increase is approximately linear (see Figure 42). On the

other hand, on the surface with NCC fibers due to presence of negative charges on the NCC, adsorption was not observed until pH 2 where strong adsorption was observed (see Figure 43). These results might be explained by the diffusive double layer around the silica particles which is highly affected by pH and NaCl concentration [16]. The isoelectric point of silica is around pH 2 and at this point the silica surface has not net charge. [16]. It is therefore likely as a consequence of this that maximum adsorption of silica would be adsorbed around pH 2. In other words, at pH 2, radius of double layers around the colloidal silica particles is at minimum and the uncharged silica can be adsorbed between the negatively charged NCC fibers on the surface. Above the isoelectric point the negatively NCC would hence repel the silica from adsorbing to the surface. A model of these two scenarios is schematically illustrated in Figure 61-62.

There are examples of studies in literature where the interaction between silica and cellulose has been studied mainly due to a rising interest in of organic-inorganic composites. E. Kontturi et al. studied the interactions between a spin coated NCC layer and the silica surface and compared this interaction (in silica/NCC) with interactions in titania/NCC system and cellulose/NCC system by the help of AFM, XPS, contact angle measurement, etc. [57]. They concluded that electrostatic repulsion between NCC and an anionic silica surface dictate the aggregation rate of NCC during spin coating and the height, the rate and the morphology of adsorbed NCC depend on this electrostatic force. Silica/cellulose interactions was also studied by Pinto et al. were they covered cellulose fibers with inorganic particles and also silica [58].

In short, the literature and this QCM-D experimental work suggest that decreasing pH in a silica/NCC composite gel may result in a stronger network in the gel due to the lower repulsion forces between NCC and silica particles at lower pHs; although, referring to pseudo-phase diagram at pH 4 (Figure 19-22) it may cause a delay in the gelation process.

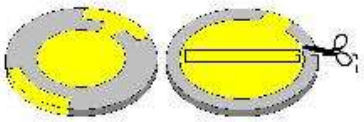

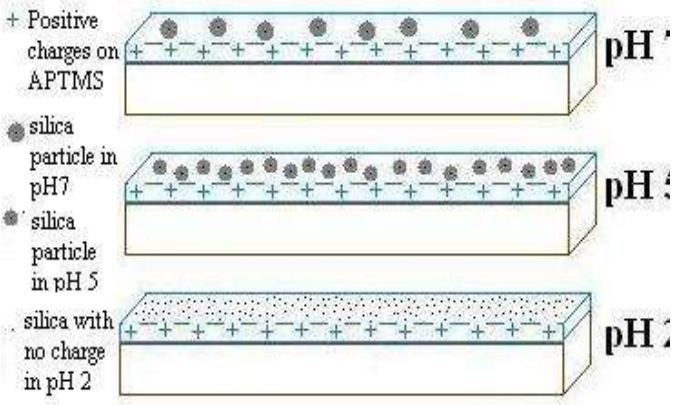

Figure 61 Adsorption of silica in three different pHs on APTMS surface with positive charge

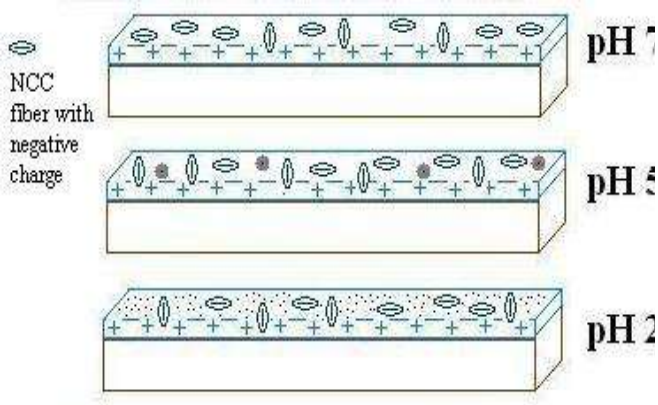

Figure 62 Adsorption of silica in three different pHs on APTMS coated with negatively charged NCC

5.3. Diffusion in gels

It was hypothesized in the beginning of the study that silica and silica/NCC gels with varying pH, particle concentrations and electrolyte levels would create different micro/nano-structures and consequently exhibit different mass transfer properties. However, it should be noted that different structures do not necessarily result in different mass transfer properties and in this study, diffusion coefficient. In the current study four different factors was investigated: silica and/or NCC concentration, pH and NaCl concentration. The diffusion coefficient was measured in 16 different gels and three controls with 1H-NMR method (table 1). In this study the measured diffusion coefficients in the gels range between 1.96×10^{-9} and 2.17×10^{-9} m^2/s. Interpretation of this difference will be described below by the help of a theoretical study of diffusion in an obstructed medium and other related studies.

The first parameter to consider is the silica concentration. Theoretically, in the case of spherical diffusion is obstructed according to the equation (7) [59]:

Here, D is the observed self-diffusion coefficient, Ø excluded volume (volume fraction) and D_0 the self-diffusion coefficient in absence of obstruction.

Figure 63 shows self-diffusion coefficient theoretically (lines) and experimentally (points) at two different salt concentration. The experimental result had a linear decrease in self-diffusion with increasing volume fraction. Furthermore, it can be seen that gels with both 0.5 and 0.9 M NaCl had a self-diffusion that experimentally decreased more than expected according to theory.

This deviation between theory and measured values was likely due to two reasons. The first reason is the effect of surface interactions between water and silica and/or NCC particles on the Brownian motion of water molecules which would decrease the self-diffusion coefficient in the gels by binding the water to the surface. The second reason could be necking between particles because of Oswald ripening and consequently a change in the overall shape of particles from the spherical to a more cylindrical shape (an assumption in the theoretical curve). If this was the case the network would obstruct the diffusion as a mixture between spheres and cylinders as described in Figure 1; however, the effect of the binding of water to the silica surface was likely to be the dominant factor as not much necking was observed in the TEM images.

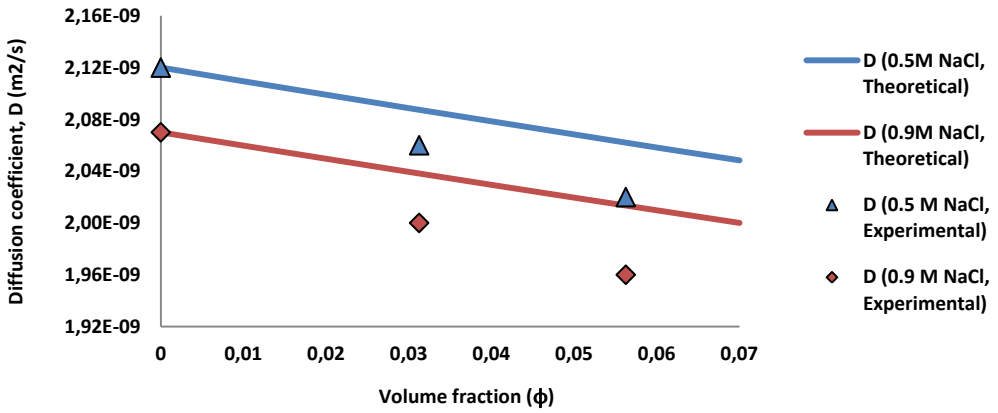

Figure 63 Diffusion in spherical particle gel. Experimental is compared with theoretical values

Regarding the impact of pH, maximum diffusion was found in pH 4. A simple comparison between diffusion coefficients in the three different pHs is illustrated in Figure 58 and it indicates that lowering the pH, increases the diffusion in the gels; however, in this study no significant difference in structure could be seen from TEM results. Although, in literature L. Hench et al. reviewed studies about the influence of acid/base on the silica gel network[33]. Accordingly, they indicated that under acidic conditions (pH 4 and pH 6) polymerization of silica results in more linear gel network

structures. In contrast, basic conditions (pH 7.8) results in a more branched network [33]. Such structure differences could not be observed in the TEM images as described before, but if they were present in a way not visually the naked eye it might be reasonable explanation for the results. Hence, more linear structures at more basic pHs provides bigger pores and self-diffusion might therefore increase. This result is also consistent with a TEM study that was conducted by M. Titulaer et al. [60] which will be discussed later in part of TEM.

Salt concentration also changes the self-diffusion and increasing NaCl concentration decreases the self-diffusion coefficient in the gels (Figure 63). This change is not only in the gels but also occurs in only salty water. O. Bernard et al. [61] calculated self-diffusion in electrolyte solutions theoretically based on long-range coulomb interactions and their theory correlate with available experimental data from this study, especially for low salt concentrations. They measured this decrease for both LiCl and NaCl [61]. Hence, the presence of NaCl itself lowers the diffusion coefficient.

Addition of NCC also lowers diffusion but silica concentration had larger impact on the diffusion because volume fraction of silica is much larger compared to the NCC volume fraction. For instance at pH 7.8 with constant silica and salt concentrations, varying NCC concentration from 0.01 wt% to 0.1 wt% (0.1-1.0 g/l) changed self-diffusion with 0.5 % which is very low. Density of silica and NCC particles are 1.65 and 1.46 respectively[55, 62] therefore, volume fractions are between 3 and 5.6 vol% for silica and between 0.007 and 0.07 vol% for NCC which it means that volume fractions of NCC is about 1-2% of total existing particles. The volume fraction of NCC was relatively low for the diffusometry measurements, but it did seem to have a small effect on diffusion and going from 0.1-1 g/l resulted in a difference in diffusion constant of 0.01 m^2/s for four different samples. This ΔD was very small and might have been because of uncertainty in the measurement, however if it is assumed to be a real difference some interesting calculations can be made. The ratio becomes 0.016 and if we do the same calculations for silica going from 5-9 wt % the corresponding ratio was . It seems that both particles have approximately the same effect per unit volume fraction on diffusion. This was a slightly unexpected result since NCC with its cylindrical shape could have been slightly more efficient to obstruct the diffusion. It is also surprising when considering that the different surface chemistry found at a NCC surface compared to a silica surface. One explanation could be that the effect on diffusion by shape and hence aspect ratio was compensated by the differences in surface chemistry. Hence NCC and silica is equally efficient at obstructing diffusion for the same change in volume fraction.

5.4. Gel structures in TEM images

One of the purposes with this study was to get a better understanding of the relation between micro/nano-structure and the transport properties (diffusion coefficient). Silica concentration was constant in 9 wt% in all TEM images (Figure 44-57). By visual checking, no significant differences between structures are distinguishable and all TEM images show more or less a similar nano/micro

structure. In some samples with higher normalized diffusion coefficients, slightly lower dispersion of silica particles and larger pores possibly could be seen.

It should be noted that visual comparison showed that the gels have great similarities in structure even though they gelled at relatively different condition in regards to pH and salt concentration. A gel system that behaves likes this could be said to be a "*robust system"* as different gelling conditions tend to result in similar micro/nano structure. It is expected that changes in silica concentration will most likely give differences in the microstructure that would be visible for the eyes, however because of experimental time constraints results for other silica weight percentages is not available for this thesis.

5.6. Suggested studies in the future work

- Effect of particle size (silica or/and NCC) on aggregation and micro/nano structure and permeability of created gels because it may cause different 3D structure with different diffusion coefficients [19, 27].
- Systematic TEM image analysis and simulation to distinguish the structure evolution, final structure differences and porosity [60, 63-65].
- Characterization the structural changes during gelation process and gel points by *small-angle static/dynamic light scattering* (optical density) methods [20, 32, 66] or *small-angle X-ray scattering* [17, 28].

Conclusion

This study presents an investigation of the pseudo-phase behavior for silica and/or NCC particle gels in different silica and NCC concentrations, pHs and NaCl concentrations. Kinetics of gelation has been studied. Aggregation terminates at the gel point after which the gels started to shrink and in some cases phase separate.

Minimum silica and NaCl concentrations needed for a gel to form in the present colloidal silica system were approximately 3wt% and 0.3 M NaCl.

Gel formation at pH 4 exhibits a significant delay for the gel formation comparing to gel formation at pH 6 or pH 7.8. This result confirms Iler's well known figure but there is a small shifting of the relative minimum gelation time to a slightly higher pH compared to the Iler figure. The reason for this phenomenon was described as a change in the balance between collision and reaction potential between silica particles.

The phase behavior of both the silica and silica/NCC systems showed that there are probably two steps in the gelation process. These two steps are aggregation and then followed by interconnection; i.e., the first step result phase separation and the second step result gel (or semi-gel).

In the presence of NCC an increase in viscosity were observed. We chose to term these solutions a 'viscous phase'. The reason for the high viscosity of these systems is the very large effective volume fraction of NCC fibers. In the silica/NCC system viscous and semi-gel behaviors were transient and several samples with the viscous and semi-gel behaviors also decreased over the time, most likely due to the slow formation of covalent bonds between silica particles. A comparison between minimum required salt concentration in the pure silica system and silica/NCC system with 5 wt% silica and pH 7.8, shows that with NCC the minimum salt concentration for gelation decreased from 0.5 M to 0.25 M:

Shrinkage was also commonly noted in the silica pseudo-phase diagram which was a result of new connections and bond formation after the gel point, an effect called Oswald ripening. Shrinkage causes contraction of the gel network and resulting expulsion of liquid from the gel pores.

The interaction between colloidal silica and NCC fibers was studied at different pH and silica concentrations with the QCM-D method. NCC covered QCM-D crystals were exposed to colloidal silica dispersions. As a control, surfaces covered with positively charged APTMS were used. When exposing the surfaces to colloid silica dispersions at different pH, adsorption to the APTMS surface differed and the results was explained by the diffusive double layer around the silica particles which was highly affected by pH and NaCl concentration. The isoelectric point of silica is around pH 2 and at this point the silica surface has not net charge; therefore maximum adsorption of silica would be

adsorbed around pH 2. In other words, at pH 2, radius of double layers around the colloidal silica particles is at minimum and the uncharged silica can be adsorbed between the negatively charged NCC fibers on the surface.

NMR diffusometry was performed in order to measure self-diffusion coefficient of water in the gels. The effect of silica and/or NCC concentration, pH and NaCl concentration were investigated. In this study the measured diffusion coefficients in the gels range between 1.96×10^{-9} and 2.17×10^{-9} m^2/s. The D-values decrease linearly with increasing volume fraction. Furthermore, it can be seen that gels with both 0.5 and 0.9 M NaCl had a self-diffusion that decreased more than expected according to theory. The deviation is likely due to two reasons: first, surface interactions between water and silica and/or NCC particles on the Brownian motion of water molecules which would decrease the self-diffusion coefficient in the gels. Secondly necking between particles because of Oswald ripening, changes in the shape of the particles from the spherical shape to a more cylindrical shape that was slightly more efficient at hindering diffusion. It is however believed that the former explanation is the most important in this context.

Lowering the pH increases the water diffusion rate. It is known that acidic conditions (pH 4 and pH 6) results in more linear gel network structures. In contrast, basic conditions (pH 7.8) results in a more branched network. Although we note that this does not explain our experiment diffusion results. NaCl concentration also changes the self-diffusion and increasing NaCl concentration decreases the self-diffusion coefficient in the gels. This is however easily explained by ‘simple’ ion hydration, an effect that slows down the water due to formation of large water-ion clusters.

Obstructing effects of NCC fibers and silica particle are almost equal for the same change in volume fraction (with the assumption that the small difference in diffusion coefficient values is not an error).

TEM images showed that the gel display fairly similar structure even though they have gelled at relatively different condition (pH and salt concentration). A gel system that behaves likes this could be said to be a “*robust* in the sense that it is not easy to change the microstructure of the material. In a sense, a material like this is very good as a model system for mass transport measurements. In the work to follow this thesis the gels investigated here will for that reason be used for flow measurements. The main goal is to correlate details in mass transport properties to details in microstructure.

Acknowledgments

*I greatly thank **Christoffer Abrahamsson**, supervisor of this project and **Magnus Nydén**, examiner of this thesis and director of SuMo organization. **Lars Nordstierna** and **Annika Altskär** are thanked for their help in my experimental work as well as **Adele Khavari** for our discussions.*

References

1. *SuMo Homepage. September 2011; Available from: http://www.chalmers.se/chem/sumo-en/.*
2. *Robinson, B.H., Self-assembly. 2003, Amsterdam ; Washington, DC, Tokyo: IOS Press ; Ohmsha. xiii, 465 p.*
3. *Philibert, J., Adolf Fick and diffusion equations. Diffusion in Solids - Past, Present and Future, 2006. 249: p. 1-6.*
4. *De Santis, S., et al., Anisotropic anomalous diffusion assessed in the human brain by scalar invariant indices. Magn Reson Med, 2011. 65(4): p. 1043-52.*
5. *Pfeuffer, J., et al., Restricted diffusion and exchange of intracellular water: theoretical modelling and diffusion time dependence of H-1 NMR measurements on perfused glial cells. Nmr in Biomedicine, 1998. 11(1): p. 19-31.*
6. *Mckean, H.P., Nelson,E - Dynamical Theories of Brownian Motion. American Scientist, 1967. 55(4): p. A517-&.*
7. *Loren, N., et al., Dendrimer Diffusion in kappa-Carrageenan Gel Structures. Biomacromolecules, 2009. 10(2): p. 275-284.*
8. *Johnsson, A.C.J.H., M.C. Camerani, and Z. Abbas, Combined Electrospray-SMPS and SR-SAXS Investigation of Colloidal Silica Aggregation. Part I. Influence of Starting Material on Gel Morphology. Journal of Physical Chemistry B, 2011. 115(5): p. 765-775.*
9. *Hamley, I.W., Introduction to soft matter : synthetic and biological self-assembling materials. Rev. ed. 2007, Chichester, England ; Hoboken, NJ: John Wiley & Sons. vii, 328 p.*
10. *Bergna, H.E., American Chemical Society. Division of Colloid and Surface Chemistry., and American Chemical Society. Meeting, The Colloid chemistry of silica : developed from a symposium sponsored by the Division of Colloid and Surface Chemistry, at the 200th National Meeting of the American Chemical Society, Washington, DC, August 26-31, 1990. Advances in chemistry series,. 1994, Washington, DC: American Chemical Society. xvii, 695 p.*
11. *DeRocher, J.P., et al., Barrier membranes with different sizes of aligned flakes. Journal of Membrane Science, 2005. 254(1-2): p. 21-30.*
12. *Akzonobel Homepage, Colloidal Silica. September 2011; Available from: http://www.akzonobel.com/colloidalsilica/about_us/learn/questions_and_answers/index.aspx#1.*
13. *Flanigen, E.M., et al., Silicalite, a New Hydrophobic Crystalline Silica Molecular-Sieve. Nature, 1978. 271(5645): p. 512-516.*
14. *International Union of Pure and Applied Chemistry. August 2011; Available from: http://www.iupac.org/nao.*
15. *Russel, W.B., D.A. Saville, and W.R. Schowalter, Colloidal dispersions. Cambridge monographs on mechanics and applied mathematics. 1989, Cambridge ; New York: Cambridge University Press. xvii, 525 p., [1] leaf of plates.*
16. *Iler, R.K., The chemistry of silica : solubility, polymerization, colloid and surface properties, and biochemistry. 1979, New York: Wiley. xxiv, 866 p.*
17. *Zukoski, C.E. and W.E. Smith, Aggregation and gelation kinetics of fumed silica-ethanol suspensions. Journal of Colloid and Interface Science, 2006. 304(2): p. 359-369.*

18. *Frolov, Y.G. and N.A. Shabanova, Factors of Aggregative Stability of Silica Hydrosols. Langmuir, 1987. 3(5): p. 640-644.*

19. *Borkovec, M., et al., Aggregation and charging of colloidal silica particles: Effect of particle size. Langmuir, 2005. 21(13): p. 5761-5769.*

20. *Bergenholtz, J., et al., Concentration effects on irreversible colloid cluster aggregation and gelation of silica dispersions. Journal of Colloid and Interface Science, 2006. 301(1): p. 137-144.*

21. *Tanaka, H., Y. Nishikawa, and T. Koyama, Network-forming phase separation of colloidal suspensions. Journal of Physics-Condensed Matter, 2005. 17(15): p. L143-L153.*

22. *Scherer, G.W., Mechanics of Syneresis .1. Theory. Journal of Non-Crystalline Solids, 1989. 108(1): p. 18-27.*

23. *Klemm, D., et al., Cellulose: Fascinating biopolymer and sustainable raw material. Angewandte Chemie-International Edition, 2005. 44(22): p. 3358-3393.*

24. *Cohen, Y., L. Avram, and L. Frish, Diffusion NMR spectroscopy in supramolecular and combinatorial chemistry: An old parameter - New insights. Angewandte Chemie-International Edition, 2005. 44(4): p. 520-554.*

25. *Q-sence Company Homepage. September 2011; Available from: http://www.q-sense.com/applications.*

26. *Hasani, M., et al., Cationic surface functionalization of cellulose nanocrystals. Soft Matter, 2008. 4(11): p. 2238-2244.*

27. *Higashitani, K., M. Kondo, and S. Hatade, Effect of Particle-Size on Coagulation Rate of Ultrafine Colloidal Particles. Journal of Colloid and Interface Science, 1991. 142(1): p. 204-213.*

28. *Zackrisson, A.S., J.S. Pedersen, and J. Bergenholtz, A small-angle X-ray scattering study of aggregation and gelation of colloidal silica. Colloids and Surfaces a-Physicochemical and Engineering Aspects, 2008. 315(1-3): p. 23-30.*

29. *Sandkuhler, P., J. Sefcik, and M. Morbidelli, Kinetics of gel formation in dilute dispersions with strong attractive particle interactions. Adv Colloid Interface Sci, 2004. 108-109: p. 133-43.*

30. *Sefcik, J., et al., Kinetics of aggregation and gelation in colloidal dispersions. Chemical Engineering Research & Design, 2005. 83(A7): p. 926-932.*

31. *Watillon, J.D.a.A., The stability of amorphous colloidal silica. Journal of colloid and interface science, 1970. 33(July 1970): p. 430-438.*

32. *Glatter, O., et al., Small-angle static light scattering of concentrated silica suspensions during in situ destabilization. Journal of Colloid and Interface Science, 2004. 271(2): p. 388-399.*

33. *Hench, L.L. and J.K. West, The Sol-Gel Process. Chemical Reviews, 1990. 90(1): p. 33-72.*

34. *Allen, L.H. and Matijevi.E, Stability of Colloidal Silica .I. Effect of Simple Electrolytes. Journal of Colloid and Interface Science, 1969. 31(3): p. 287-&.*

35. *Depasse, J., Coagulation of colloidal silica by alkaline cations: Surface dehydration or interparticle bridging? Journal of Colloid and Interface Science, 1997. 194(1): p. 260-262.*

36. *Johnson, A.C.J.H., et al., Aggregation of Nanosized Colloidal Silica in the Presence of Various Alkali Cations Investigated by the Electrospray Technique. Langmuir, 2008. 24(22): p. 12798-12806.*

37. *Bremer, L.G.B., P. Walstra, and T. Vanvliet, Estimations of the Aggregation Time of Various Colloidal Systems. Colloids and Surfaces a-Physicochemical and Engineering Aspects, 1995. 99(2-3): p. 121-127.*

38. *Singh, G. and L.F. Song, Experimental correlations of pH and ionic strength effects on the colloidal fouling potential of silica nanoparticles in crossflow ultrafiltration. Journal of Membrane Science, 2007. 303(1-2): p. 112-118.*

39. *Habibi, Y., L.A. Lucia, and O.J. Rojas, Cellulose nanocrystals: chemistry, self-assembly, and applications. Chem Rev. 110(6): p. 3479-500.*

40. *Araki, J. and S. Kuga, Effect of trace electrolyte on liquid crystal type of cellulose microcrystals. Langmuir, 2001. 17(15): p. 4493-4496.*

41. *Jin, H., et al., Nanofibrillar cellulose aerogels. Colloids and Surfaces a-Physicochemical and Engineering Aspects, 2004. 240(1-3): p. 63-67.*

42. *Olsson, R.T., et al., Making flexible magnetic aerogels and stiff magnetic nanopaper using cellulose nanofibrils as templates. Nature Nanotechnology, 2010. 5(8): p. 584-588.*

43. *Aulin, C., et al., Nanoscale Cellulose Films with Different Crystallinities and Mesostructures-Their Surface Properties and Interaction with Water. Langmuir, 2009. 25(13): p. 7675-7685.*

44. *Dong, X.M., et al., Effects of ionic strength on the isotropic-chiral nematic phase transition of suspensions of cellulose crystallites. Langmuir, 1996. 12(8): p. 2076-2082.*

45. *Ono, H., et al., H-1-NMR relaxation of water molecules in the aqueous microcrystalline cellulose suspension systems and their viscosity. Cellulose, 1998. 5(4): p. 231-247.*

46. *Celzard, A., V. Fierro, and R. Kerekes, Flocculation of cellulose fibres: new comparison of crowding factor with percolation and effective-medium theories. Cellulose, 2009. 16(6): p. 983-987.*

47. *Dzolic, Z., K. Wolsperger, and M. Zinic, Synergic effect in gelation by two-component mixture of chiral gelators. New Journal of Chemistry, 2006. 30(10): p. 1411-1419.*

48. *Frkanec, L. and M. Zinic, Chiral bis(amino acid)- and bis(amino alcohol)-oxalamide gelators. Gelation properties, self-assembly motifs and chirality effects. Chemical Communications, 2010. 46(4): p. 522-537.*

49. *Sugiyasu, K., et al., Double helical silica fibrils by sol-gel transcription of chiral aggregates of gemini surfactants. Chemical Communications, 2002(11): p. 1212-1213.*

50. *Numata, M., et al., Sol-gel reaction using DNA as a template: An attempt toward transcription of DNA into inorganic materials. Angewandte Chemie-International Edition, 2004. 43(25): p. 3279-3283.*

51. *Sugiyasu, K., N. Fujita, and S. Shinkai, Fluorescent organogels as templates for sol-gel transcription toward creation of optical nanofibers. Journal of Materials Chemistry, 2005. 15(27-28): p. 2747-2754.*

52. *Morbidelli, M., M. Soos, and J. Sefcik, Investigation of aggregation, breakage and restructuring kinetics of colloidal dispersions in turbulent flows by population balance modeling and static light scattering. Chemical Engineering Science, 2006. 61(8): p. 2349-2363.*

53. *Scherer, G.W., Mechanics of Syneresis .2. Experimental-Study. Journal of Non-Crystalline Solids, 1989. 108(1): p. 28-36.*

54. *Okiyama, A., et al., Bacterial Cellulose .1. 2-Stage Fermentation Process for Cellulose Production by Acetobacter-Aceti. Food Hydrocolloids, 1992. 6(5): p. 471-477.*

55. *Sun, C.Q., True density of microcrystal line cellulose. Journal of Pharmaceutical Sciences, 2005. 94(10): p. 2132-2134.*

56. *Abe, K. and H. Yano, Formation of hydrogels from cellulose nanofibers. Carbohydrate Polymers, 2011. 85(4): p. 733-737.*

57. *Kontturi, E., et al., Cellulose nanocrystal submonolayers by spin coating. Langmuir, 2007. 23(19): p. 9674-9680.*

58. *Pinto, R.J.B., et al., Novel SiO2/cellulose nanocomposites obtained by in situ synthesis and via polyelectrolytes assembly. Composites Science and Technology, 2008. 68(3-4): p. 1088-1093.*

59. *Nilsson, P.G. and B. Lindman, Water Self-Diffusion in Non-Ionic Surfactant Solutions - Hydration and Obstruction Effects. Journal of Physical Chemistry, 1983. 87(23): p. 4756-4761.*

60. *Titulaer, M.K., et al., Microscopic Shrinkage Free Silica-Gels by Electrodialysis. Journal of Non-Crystalline Solids, 1994. 171(2): p. 123-133.*

61. *Bernard, O., et al., Self-Diffusion in Electrolyte-Solutions Using the Mean Spherical Approximation. Journal of Physical Chemistry, 1992. 96(1): p. 398-403.*

62. *Eka Chemicals Homepage: Bindzil GB Colloidal Silica Dispersions. September 2011; Available from: http://www.akzonobel.com/colloidalsilica.*

63. *Babu, S., J.C. Gimel, and T. Nicolai, Self-diffusion of reversibly aggregating spheres. Journal of Chemical Physics, 2007. 127(5).*

64. *Gimel, J.C. and T. Nicolai, Self-diffusion of non-interacting hard spheres in particle gels. Journal of Physics-Condensed Matter, 2011. 23(23).*

65. *Babu, S., et al., The influence of bond rigidity and cluster diffusion on the self-diffusion of hard spheres with square well interaction. Journal of Chemical Physics, 2008. 128(20).*

66. *Zackrisson, M., et al., Small-angle neutron scattering on a core-shell colloidal system: a contrast-variation study. Langmuir, 2005. 21(23): p. 10835-45.*